water

MDPI

Article

Selection of C~~I~~MIP5 GCM ensemble for the projection of ~~spatio~~Spatio-temporal changes in precipitation and temperature over the Niger Delta, Nigeria.

Ibrahim Hassan[1,2]*, Robert M. Kalin[1], Christopher J. White[1], Jamiu A. Aladejana[1,3]

1 Department of Civil and Environmental Engineering, University of Strathclyde, Glasgow, UK; Ibrahim.hassan@strath.ac.uk, Robert.Kalin@Strath.ac.uk, chris.white@strath.ac.uk,
2 Department of Civil Engineering Abubakar Tafawa Balewa University Bauchi, Nigeria;
3 Department of Geology, University of Ibadan, Nigeria; jamiu.aladejana@strath.ac.uk
* Correspondence:Correspondence: Ibrahim.hassan@strath.ac.uk; Tel.: (+447770028315)

Formatted: Font color: Auto

Formatted: Font color: Auto

Received: date; Accepted: date; Published: date

Abstract: Selection of a suitable General Circulation Model (GCM) ensemble is crucial for effective water resources management and reliable climate studies in developing countries with constraint in human and computational resources. A careful selection of a GCM subset by excluding those with limited similarity to the observed climate from the existing pool of GCMs developed by different modeling centers at various resolutions can ease the task and minimize uncertainties. In this study, a feature selection method known as symmetrical uncertainty (SU) was employed to assess the performance of 26 Coupled Model Intercomparison Project Phase 5 (CMIP5) GCM outputs under Representative Concentration Pathway (RCP) 4.5 and 8.5. The selection was made according to their capability to simulate observed daily precipitation (prcp), maximum and minimum temperature (Tmax and Tmin) over the historical period 1980–2005 in the Niger Delta region which is highly vulnerable to extreme climate events. The ensemble of the four top-ranked GCMs, namely ACCESS1.3, MIROC-ESM, MIROC-ESM-CHM and NorESM1-M, were selected for the Spatio-temporal projection of prcp, Tmax and Tmin over the study area. Results from the chosen ensemble predicted an increase in the mean annual prcp between the range of 0.26% to 3.57% under RCP 4.5, and 0.7% to 4.94% under RCP 8.5 by the end of the century when compared to the base period. The study also revealed an increase in Tmax in the range of 0 to 0.4 °C under RCP4.5 and 1.25-1.79 °C under RCP8.5 during the periods 2070 – 2099. Tmin also revealed a significant increase of 0 to 0.52 °C under RCP4.5 and between 1.38-2.02 °C under RCP8.5, which shows that extreme events might threaten the Niger Delta due to climate change. Water resource managers in the region can use these findings for effective water resources planning, management and adaptation measures.

~~For effective planning and management of water resources, selection of a suitable GCMs ensemble is crucial for any reliable future climate change studies which can be very challenging due to the existence of many GCMs from different modeling centers at various resolutions and uncertainties. Thus, they can be minimized by careful selection. The performance of GCMs is generally assessed according to their capability to simulate observed historical precipitation (pcp), maximum and minimum temperature (Tmax and Tmin) of a defined region. In this study, a feature selection method known as symmetrical uncertainty (SU) was used for the assessment and ranking of 26 Coupled Model Intercomparison Project Phase 5 (CMIP5) GCMs based on their ability to simulate daily precipitation, maximum and minimum temperature over the historical period 1980–2005. The performance of GCMs in identifying a suitable ensemble was assessed using gridded climate data obtained from Climatic Research Unit (CRU) as observed datasets. The ensembles of the four top-ranked GCMs was considered for the projection of the region's climate. The biases in raw GCMs~~

~~were correct using Additive correction factor for temperature and multiplicative correction factor for precipitation. The top four GCMs namely ACCESS1.3, MIROC ESM, MIROC ESM CHM and NorESM1-M were selected for the Spatio-temporal projection of pcp, Tmax and Tmin over the Niger Delta. The ensemble chosen for the regions climate projection revealed a decrease in the mean annual precipitation between 19–23% under RCP4.5 and 13–19 % under RCP8.5 during the period 2070 – 2099 when compared to the base period. The study also reveals an increase in Tmax in the range of 0.9 °C – 1.95 °C under RCP4.5 and 3.6 °C – 3.8 °C under RCP8.5 during the periods 2070 – 2099. Tmin is also expected to increase significantly by 2.25 °C under RCP4.5 and between 3.6 °C – 3.8 °C under RCP8.5. These findings can be used by water resource managers for effective mitigation planning and management of water resources over the Niger Delta.~~

Keywords: Global Climate Models; Niger Delta; Coupled Model Intercomparison Project Phase 5; Respectively Concentration Pathways; Symmetrical Uncertainty; Temperature; Precipitation; Gridded Dataset

Formatted: MDPI_1.7_abstract

1. Introduction

General Circulation Models (GCMs) are numerical ~~mathematical~~ representations of the atmosphere, ocean, and land surface processes developed based on physical laws and physical-based empirical relationships. GCMs simulations are essential tools for assessing the impact of climate change for a range of human and natural systems [1]. The simulated GCM outputs~~s climate~~ ~~is~~are associated with uncertainties (e.g. due to model resolution, ~~parametrisation,~~ assumption, or calibration processes e.t.c [2–10] that hinder GCM~~s~~ outputs from ~~modelling~~ accurately projecting future climate ~~projections~~ at a regional or local level. To reduce ~~this~~ these ~~uncertainty~~uncertainties, a subset of GCMs may be selected to caveat ~~for~~ a given study area by excluding those w~~hich have~~ith limited similarity to the observed climate [6,8,11–13]. ~~This subset selection can, however, be very challenging due to the existence of many GCMs from different modelling centres at various resolutions and uncertainties.~~ These uncertainties can be minimised by a careful selection of an ensemble model for climate projection [14]. It is also practically not feasible to use all the CMIP5 GCMs for climate change projection and impact assessment due to constraint in human and computational resources [15]. A small ensemble of more appropriate GCMs is selected for any region of interest by excluding those considered unrealistic and in order to reduce the spread of uncertainties associated with GCM [11].

The selection of a GCM ensemble subset requires an approach tailored towards the efficacy of the model dependence or performance in climate projection impact analyses [16]. Existing methods generally follow two approaches: (i) the ‘past performance approach’, which is based on a GCMs ability to replicate historical climate but does not take into account the future projection [17], and (ii) the ‘envelope approach’, which selects GCMs according to their agreement in the future climate projections but does not consider a GCMs ability to replicate the past climate [18]. The combination of the past performance approach with the envelope method is referred to as the ‘hybrid approach’. The past performance approach produces ~~more realistic~~better projections when employed for identifying an ensemble from a large pool of GCMs, suggesting that the past performance evaluation is a suitable approach because the ability of a GCM to simulate the past climatic conditions suggests it may also ~~therefore~~, therefore, be more likely to predict the future climate with increased accuracy [8,11,19,20].

Formatted: Font: (Asian) 宋体

A GCM ensemble produced by the past performance approach is usually assessed by comparing historical observed climatic variables with the simulated GCM variables over a baseline period [19]. Three algorithms known as ‘filters’, ‘wrappers’ and the ‘hybrid’ of filters and wrappers have been used by the past performance approach in the selection of the GCMs subset by ranking the GCMs concerning a climate variable(s) based on their past performance [11,21]. These three algorithms are also referred to as ‘Feature selection methods’. The filter's algorithm select an ensemble of GCMs based on their derived scores from various statistical tests such as correlation coefficient, significance tests, linear discriminant analysis, and information gain [22–25]; while wrappers algorithm, in contrast, select an ensemble of GCMs by employing iterative learning algorithms such as forward selection, recursive variable elimination and greedy search [12,26]. Hybrids of filters and wrappers are used to identify better performing GCMs from an initially filtered ensemble of GCMs [12,27]. The major drawback of filters is that they ignore inter-dependencies among GCM~~s~~ output for a given variable and therefore, may select inappropriate GCMs for the ensemble. Wrappers are also computationally intensive and also often found to choose ~~inappropriate~~ the best set of GCMs due to overfitting of the regression model [11,12]. The hybrids of filters and wrappers are computationally less intense compared to wrappers but found to perform ~~similarly to wrappers~~ better when used on a large number of GCMs [11,15,28]. ~~Hybrids of filters and wrappers are more suitable to be used with a large number of GCMs [11,15].~~

Many studies have been conducted to determine the performance of GCM outputs by~~s~~ employing various wrappers and filters in respect to gridded data which include; clustering hierarchy [14], weighted skill score [29], spectral analysis [30], Bayesian weighting [31], and information entropy [32]~~, have been used for the above purpose~~. Various statistical indicators such as correlation coefficients [23] have also been used for GCM evaluation, ranking and selection. The disadvantage~~s~~ of using ~~these~~ statistical indicators such as correlation coefficients is that their performance matrices are also mostly evaluated based on the mean climatic condition ~~state of the climatic condition~~ where temporal variability ~~such as trends or seasonal variability~~ of the climate is not given full attention [33].

Several studies have recently used the feature selection methods ~~to~~ in selecting the most suitable GCM~~s to form an~~ ensemble subset for climate studies and projection in different areas around the world. Symmetrical uncertainty (SU) is a feature selection method which measures changes in entropy based on the concept of information entropy in other to assess the similarity or mutual information between GCM and observed datasets [34–36]. ~~–~~[8] used SU in the selection of GCMs for the spatiotemporal forecast of changes in temperature of Iraq. [12,19] recently used SU in selecting, ranking and assessing the performance of several GCMs in Pakistan. [20] applied a combination of Entropy Gain (EG), Gain Ratio (GR), and Symmetrical Uncertainty (SU) approach in screening the past performance and selection of rainfall GCMs in Nigeria. This study explores the use of Symmetrical Uncertainty~~SU~~ feature selection methods in selecting and ranking the most suitable GCMs to form an ensemble GCM for ~~temperature and rainfall~~Pcp, Tmax and Tmin projection in the Niger Delta part of Nigeria. The objective of this study was, therefore, to use the Symmetrical Uncertainty ~~SU~~ algorithms in identifying the most suitable GCM~~s~~ ensemble from 26 CMIP5 GCMs in reconstructing the prcp, Tmax and Tmin ~~precipitation, maximum and minimum temperature~~ over the Niger Delta for reliable climate projection. The selected GCM~~s~~ ensemble was then used for reliable prediction of climate for the Niger Delta, which is highly vulnerable to extreme climate events with large spatial and seasonal variability.

2. Materials and methods

2.1. Description of the study area

The study area is located in the Niger Delta part of Nigeria and comprises of Bayelsa and Rivers State~~. The placements of these states are presented in~~ (Figure 1). The ~~area is~~ area is low lying coastal area drained by Rivers Kwa-Ibo, Imo, Bonny, Aba, ~~Kwa-Ibo, Bonny,~~ and their ~~respective~~ tributaries. The region belongs to the equatorial climate towards the southern coast and subequatorial climate towards the northern tropical rainforest [37]. The ~~topography~~ elevation of the area under the influence of high coastal tides results in flooding, ~~mostly~~ especially during the rainy season [38]. ~~The climatic condition in the region belongs to the tropical rainforest within the wet equatorial climatic region.~~ The area is characterised by typical tropical wet (March to October) and dry seasons (November to February) with a mean annual rainfall ~~decreasing~~ increasing from 2000 mm around the northern fringe to about 4500 mm around the coastal margin ~~to about 2000 mm around the~~

Formatted: Font color: Auto

Formatted: Font color: Auto

Formatted: Font color: Auto

Formatted: Font color: Auto

Formatted: Font color: Auto

Formatted: Font color: Auto

~~northern fringe of the study area~~ [39]. A short spell of the dry season, often referred to as the 'August break' caused by the deflection of the moisture-laden current is often experienced in August ~~and sometimes occurs in July~~ or September [40] ~~due to variations in weather~~.

~~The mean monthly temperatures are higher up to 26.67 °C around March / April and as low as 24.44 °C during July/ August giving a small annual range of 2.73 °C. The mean relative humidity of the area is relatively high often reaching 90%, while the warm, wet southwesterly winds blow inland most of the year and the dust-laden, warm-dry North-easterly winds occasionally reach the coast for small periods of the year [36]. Recent trends of increase in temperature, precipitation and flood frequencies observed over the years in the Niger Delta due to global warming depicts a clear sign of climate change with a variable future climate over the region [37–40].~~

~~*2.2. Data and sources*~~

~~2.2.1. Gridded Dataset~~

~~The datasets used in this study are the Climate Research Unit (CRU) daily rainfall and temperature datasets between the historic years of 1980 to 2005 over the Niger Delta part of Nigeria due to the scarcity of reliable long records of hydroclimatological stations observations in the area. The CRU datasets are observation based gridded precipitation and temperature datasets which are widely used because of their extensive spatial and temporal coverage extracted from the CRU version 4.01 global climate dataset [41–43]. They were found to be the best fit datasets that replicate the distribution patterns, spatial and temporal variability of the Niger Delta's observed datasets [44]. The gridded datasets are re-gridded to a common spatial resolution of 0.5°X 0.5° following the agreed resolution of the GCMs. The daily CRU was downloaded as NetCDF files from [http://www.cru.uea.ac.uk] resulting in an equal number of grids (22 grids) which were spatially distributed across the study area. The observed station data had only one observation within the study area with two other contributing stations outside the study area. The historic daily climate data (precipitation (pcp), minimum and maximum temperature (Tmin, Tmax)) data within the same grid locations that house the observed meteorological station were downscaled to the station resolution. These datasets cover a period of 1980 – 2005 for the historical period as observed climate data and GCM simulated dataset covering periods of 1950–2005 for the historical periods and 2006 – 2099 for the future periods.~~

Formatted: English (United States), Check spelling and grammar

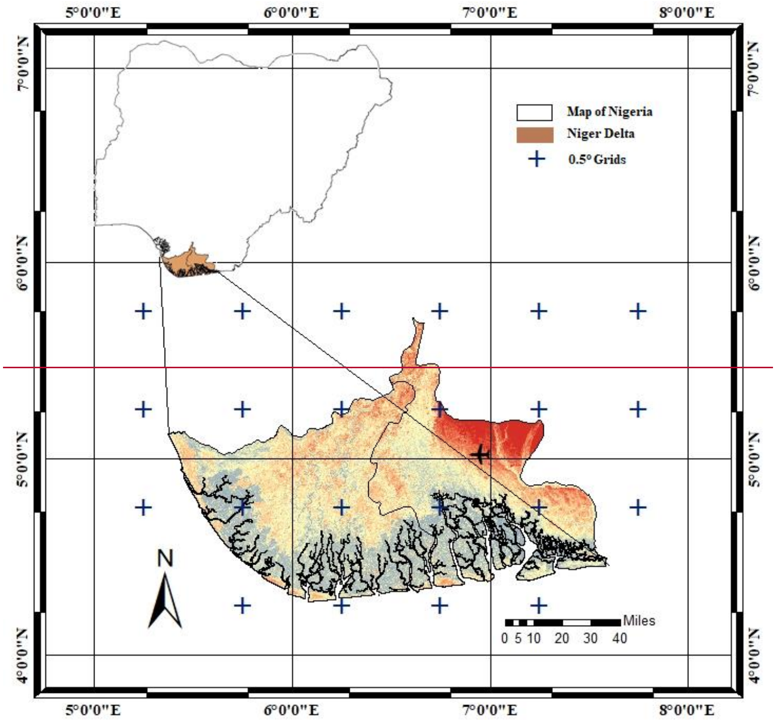

Formatted: Justified, Space Before: 12 pt

Formatted Table

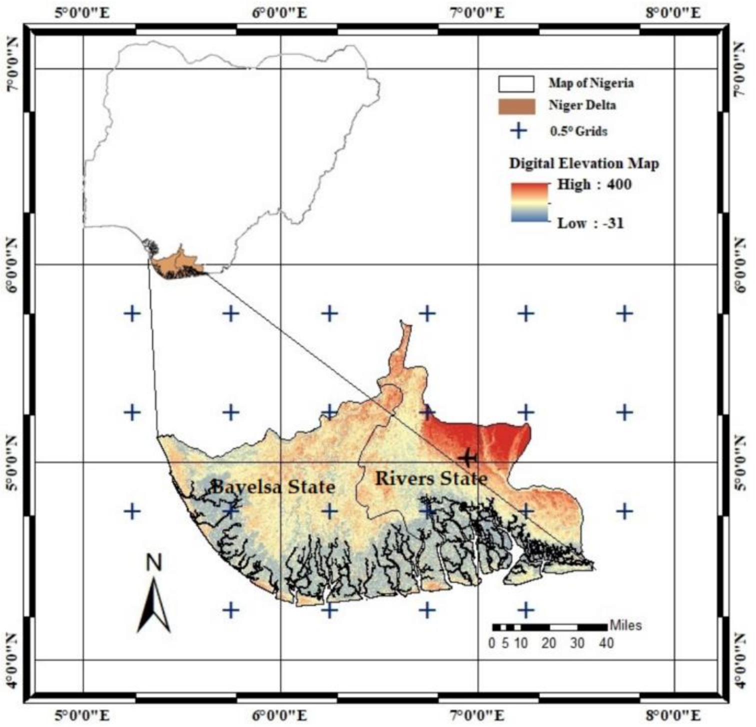

Figure 1. Map of ~~the~~ study area ~~in Nigeria~~ showing the spatial distribution of 0.5⁰ x 0.5⁰ grids.

The mean monthly temperatures are higher up to 26.67 °C around March / April and as low as 24.44 °C during July/ August giving a small annual range of 2.73 °C. The mean relative humidity of the area is relatively high often reaching 90%, while the warm, wet southwesterly winds blow inland most of the year and the dust-laden, warm-dry North-easterly winds occasionally reach the coast for small periods of the year [41]. Recent studies show that during the last 20 years [42], a trend of increase in prcp, Tmin and Tmax and flood frequencies observed over the years in the Niger Delta due to global warming depicts a clear sign of climate change with a variable future climate over the region [43–46].

Formatted: Justified, Indent: Left: 0 cm

~~2.2.2. Coupled Model Inter-comparison Project Phase 5 (CMIP5) GCM Datasets~~

~~Twenty six GCMs of ISI-MIP (Inter-sectorial impact model inter-comparison project) [45] models (Table 1) and two carbon emission scenarios (RCP4.5 and RCP8.5) for the years (1980-2099) were downscaled for the basin in other to be consistent with the CRU datasets observations. The GCM data was obtained from the CMIP5 data portal website (http://pcmdi9.llnl.gov/). The GCMs were selected based on the availability of daily simulation for two representative concentration pathways (RCP), which are RCP4.5 and RCP8.5 scenarios.~~

~~The RCP4.5 is an intermediate pathway scenario which shows a good agreement with the latest policy of lower greenhouse gas emission by the global community while the RCP8.5 is the business-as-usual scenario which provides the possible highest impact on climate change [46]. Therefore, RCP 4.5 and RCP 8.5 were selected as these two scenarios can provide a possible complete range of impact. As the GCMs are available in different resolutions, all CMIP5 data were, therefore, interpolated~~

~~uniformly to the same spatial scale (0.5º X 0.5º) to reduce biases introduced by different resolution for fair comparison using inverse distance weight (IDW) interpolation technique. This technique uses nearby areas to generate point output from each GCM at each grid point and thus provides a smooth interpolation which is widely used for re-gridding of GCMs [43]. Table 1 gives an overview of GCMs.~~

Table 1. General Circulation Models (GCMs) Used in the Study at 0.5^0 Grid.

GCM No	GCM Name	Institute	Resolution
1	ACCESS1.3	Commonwealth Scientific and Industrial Research Organisation–Bureau of Meteorology, Australia	1.9 × 1.2
2	CanCM4	Canadian Centre for Climate Modelling and Analysis, Canada	2.8 × 2.8
3	CanESM2		
4	CCSM4	National Centre for Atmospheric Research USA	0.94 × 1.25
5	CMCC.CESM	Centro Euro-Mediterraneo sui Cambiamenti Climatici, Italy	0.7 × 0.7
6	CMCC.CMS		1.9 × 1.9
7	CNRM.CM5	Centre National de Recherches Météorologiques, Centre, France	1.4 × 1.4
8	CSIRO.Mk3.6.0	Commonwealth Scientific and Industrial Research Organization, Australia	1.9 × 1.9
9	CSIRO.Mk3L.1.2		
10	GFDL.CM3	Geophysical Fluid Dynamics Laboratory, USA	2.5 × 2.0
11	GFDL.ESM2M		
12	GISS.E2.H	NASA/GISS (Goddard Institute for Space Studies), USA	2.5 × 2.0
13	HadCM3	Met Office Hadley Centre, UK	1.9 × 1.2
14	HadGEM2.AO		
15	HadGEM2.CC		
16	HadGEM2.ES		
17	INMCM4	Institute of Numerical Mathematics, Russia	2.0 × 1.5
18	IPSL.CM45A.LR	Institut Pierre Simon Laplace, France	2.5 × 1.3
19	IPSL.CM5A.MR		3.7 × 1.9
20	MIROC.ESM	The University of Tokyo, National Institute for Environmental Studies, and Japan Agency for Marine-Earth Science and Technology, Japan	2.8 × 2.8
21	MIROC.ESM.CHM		
22	MIROC5		1.4 × 1.4
23	MPI.ESM.LR	Max Planck Institute for Meteorology, Germany	1.9 × 1.9
24	MPI.ESM.MR		
25	MRI.CGCM3	Meteorological Research Institute, Japan	1.1 × 1.1
26	Noer.ESM1.M	Meteorological Institute, Norway	2.5 × 1.9

2.2. Data and sources

Formatted: Space Before: 54 pt

2.2.1. Gridded Dataset

The datasets used in this study are the Climate Research Unit (CRU) daily prcp, Tmax and Tmin datasets between the historic years of 1980 to 2005 over the Niger Delta part of Nigeria due to the scarcity of reliable long records of hydroclimatological stations observations in the area. The CRU datasets are observation-based gridded prcp, Tmin and Tmax datasets which are widely used because of their extensive spatial and temporal coverage extracted from the CRU version 4.01 global climate dataset [47–49]. They were found to be the best-fit datasets that replicate the distribution patterns, spatial and temporal variability of the Niger Delta's observed datasets [50]. The gridded datasets are re-gridded to a common spatial resolution of 0.5°X 0.5° following the agreed resolution of the GCMs. The daily CRU datasets were downloaded from [http://www.cru.uea.ac.uk] resulting in an equal number of grids (22 grids) which were spatially distributed across the study area. The observed station data had only one observation within the study area with two other contributing stations outside the study area. The historic daily climate data (prcp, Tmin and Tmax) data within the same grid locations that house the observed meteorological station were downscaled to the station resolution. These datasets cover a period of 1980 – 2005 for the historical period as observed climate data and GCM-simulated dataset covering periods of 1950–2005 for the historical periods and 2006 – 2099 for the future periods.

2.2.2. Coupled Model Inter-comparison Project Phase 5 (CMIP5) GCM Datasets

Twenty-six GCMs of ISI-MIP (Inter-sectorial impact model inter-comparison project) [51] models (Table 1) and two carbon and other greenhouse, aerosols, etc. emission scenarios (RCP4.5 and RCP8.5) for the years (1980-2099) were downscaled for the basin in other to be consistent with the CRU datasets observations. The GCM data was obtained from the CMIP5 data portal website (http://pcmdi9.llnl.gov/). The GCMs were selected based on the availability of daily simulation for two representative concentration pathways (RCP), which are RCP4.5 and RCP8.5 scenarios.

The RCP4.5 is an intermediate pathway scenario which shows a good agreement with the latest policy of lower greenhouse gas emission by the global community while the RCP8.5 is the business-as-usual scenario which is consistent with future that has no change in climate policy to reduce emissions [52]. Therefore, RCP 4.5 and RCP 8.5 were selected as these two scenarios can provide a possible complete range of impact. As the GCMs are available in different resolutions, all CMIP5 data were, therefore, extracted and downscaled uniformly to the same spatial scale (0.5° X 0.5°) to reduce biases introduced by different resolution for a fair comparison. This technique uses nearby areas to generate point output from each GCM at each grid point and thus provides a smooth interpolation which is widely used for re-gridding of GCMs [49]. Table 1 gives an overview of GCMs.

3. Methodology

The procedure for identification and ranking of a subset of ~~better performing~~ GCM~~s~~ ensemble for simulation of the spatial and temporal projection of changes in rainfall and temperature for this study are outlined as follows:

1. Extracting and re-gridding of the selected 26 GCM~~s~~ –datasets and CRU gridded datasets to a spatial resolution of $0.5^{\circ} \times 0.5^{\circ}$ was carried out.
2. SU was then applied to evaluate and assess the association between the 26 GCMs and the CRU gridded observations (prcp, Tmax and Tmin) at each of the 22 grid points of 0.5°x0.5° resolution covering the study area, (Figure 1) over the reference period ~~study period~~ 1980 – 2005.
3. The GCMs were then ranked based on the computed SU weight obtained at each grid points using the SU weighting technique, where a higher rank was given to GCMs with more weight in most of the grid points. A separate list of rank is prepared for each climatic variable (prcp, Tmax and Tmin) and each gridded dataset (Table 2).

Formatted: Justified

4. The overall GCMs ranks were then derived (equation 4) considering all their ranks and the weights obtained at all the 22 grid over the entire study area.
5. The final ranks of all the three datasets were determined ~~using a comprehensive rating metric~~ based on the frequency of occurrence of each GCM to combine the overall ranks in other to obtain a single rank for each GCM valid for the entire study.
6. For simplicity, the easiest and yet the most common method of ~~downscaling by~~ bias correction was carried out for correction of the biases in the best-selected future GCM ensemble against the CRU gridded observations. The additive correction method was used for temperature bias correction while the multiplicative correction method was used to correct the biases in ~~precipitation~~ prcp for GCM simulations under the two RCPs scenarios for the period 2010 – 2099.
7. The ensemble of the best four performing GCMs was then used for the ~~projection~~ prediction of spatial, temporal and seasonal changes in rainfall for three future periods (2010 – 2039, 2040 – 2069, and 2070–2099) against the historical period (1980 – 2005).

3.1. Model selection using symmetrical uncertainty

Symmetrical uncertainty (SU) is an information ~~entropy~~ entropy-~~theory~~ based filtering approach ~~based on the concept of information entropy [47]~~ which measures the changes in entropy based on the concept of information entropy in other to assess the similarity or mutual information ~~of~~ between GCM ~~with~~ and observed datasets [34,36]. The information entropy estimates the amount of information common between the two variables. For example, if P(X) and P(Y) are the probability density functions and P(X, Y) is the joint probability density function of A and B, then the entropy H between X and Y ~~[48,49]~~ is given in Eq. (1) ~~as~~ below [36,53]:

$$H(X,Y) = \sum P(X,Y) log \frac{P(X,Y)}{P(X).P(Y)} \qquad (1)$$

The relation of entropy and mutual information can then be used to solve the problem in different ways as follows; if H(X) denote entropy of X, then:

$$H(X) = -\int P(X) \log\big(P(X)\big)\, dx \qquad (2)$$

~~H estimates~~ The common information between the two variables is estimated by H as the difference between the sum of the entropies ~~and their joint entropy~~. The amount by which the entropy of X decreases reflects additional information about X provided by Y, and is called information gain (IG), which is given by Eq. (~~2~~3) [54]. Information gain (IG) measures how much one random variable tells about another.

$$IG(X,Y) = H(X) - H(X,Y) \qquad (\cancel{2}3)$$

~~where, H(X) and H (X, Y) denotes the entropy of X and the joint entropy of X and Y, respectively.~~

The H estimated using Equation (1) indicates the amount of mutual information between the observations and GCMs. If the variables are independent to each other, the IG is 0, while a higher value of IG indicates the GCMs has higher similarity with the gridded observations.

The IG is biased toward the variable having higher values. These biases are compensated by dividing the IG value with the sum of the entropies of the random variables, which is referred to as SU. Therefore, SU provides an unbiased estimation of the degree of similarity or dissimilarity of a GCM with the corresponding observations regardless of the shape of the underlying distributions. The SU uses the following steps for GCM selection:

$$SU(X,Y) = 2\frac{IG(X,Y)}{H(X)+H(Y)} \qquad (\cancel{3}4)$$

Formatted: Line spacing: single

where, H(X) and H(Y) denotes the conditional entropies of X and Y, while H (X, Y) represents the joint entropy of X and Y, respectively. SU values vary between 0 and 1, where 1 refers to a perfect agreement between the observations and GCMs, while a value of 0 refers to no agreement between the observations and GCMs [55].

3.2. Ranking of GCMs using the weighting method

Ranking of GCMs at a single grid point is a relatively simple task. However, assessment and classification of GCMs from multiple grid points become ~~arduous~~ difficult as the exercise may display different degrees of accuracies at different grid points. This becomes more difficult when the underlying preference model, like weights assignable to different attributes for some parameters, are considered. To overcome this challenges, a technique that aggregates and combines information from different sources such as the weighting Method [56], frequency of occurrence majority rule [57], numerical averaging [13] can be employed. In this study, the ranks of the GCMs relating to each grid point were computed for each climate variable based on the computed SU weights for the 22 grid~~s~~ points, considering all the 26 GCMs. These are then ranked based on the frequency of occurrence at different ranks [17].

Then overall weight (W_o) for each variable (i.e. P, Tmax and Tmin) and each GCM was determined by multiplying the frequency of occurrence of each GCM at a particular rank with the computed SU weight corresponding to its rank and summing all the values obtained [12] as shown in Eq. (~~4~~5) below:

$$W_o = X_1(w_1) + X_2(w_2) + X_3(w_3) \ldots\ldots\ldots + X_{28}(w_{28}) \qquad (45)$$

Formatted: Space Before: 0 pt, After: 6 pt

where X represents the frequency of occurrence (e.g. X_1 corresponds to the frequency of occurrence of GCM at rank 1), w represents the weight corresponding to each rank, and Wo denotes the overall weight of each GCM.

The ensemble~~s~~ of the four top-ranked GCMs was then considered for the simulation of daily Prcp, Tmax and Tmin.

3.3. Bias correction

Projected raw GCM typically contains biases when compared with observations [58]~~, typically~~. Bias correction was carried out to correct the projected raw GCM output using the differences in the mean and variability between GCM and observed datasets. In this study, the biases in the daily time series of the variables (i.e., prcp, Tmin and Tmax~~Pcp, tasmax, and tasmin~~) from the four top-ranked GCM outputs~~s~~ were corrected using the easiest and yet the most common methods which were the ~~Additive~~ additive method for temperature and multiplicative method for prcp [49,59,60]~~precipitation~~. For temperature, the additive correction factor for each month is used, and the adjusted formula for modified daily temperature (~~t~~T~~as~~max and ~~t~~T~~as~~min) is expressed in Eq. (~~5~~6).

$$T_{corrected_{ij}} = T_{GCM_{ij}} + \left(\bar{T}_{reference_{jk}} - \bar{T}_{GCM_{jk}}\right) \qquad (56)$$

where T is the temperature, $\bar{T}$~~T~~ is the long-term average temperature, and i, j, k are respectively day, month, and year counters. ~~-~~For ~~precipitation~~prcp, a multiplicative correction factor for each month is used, and the modified daily rainfall is expressed in Eq. (~~6~~7):

$$P_{corrected_{ij}} = P_{GCM_{ij}} * \frac{\bar{P}_{reference_{jk}}}{\bar{P}_{GCM_{jk}}} \qquad (67)$$

where P is the precipitation (mm day^{-1}), and $\bar{P}$~~P~~ is the long-term average precipitation.

3.4. Performance assessment

Performance of the ensemble~~s~~ from all the 26 GCMs~~,~~ and 4 ~~selected~~ SU selected GCMs ~~and the modified SU GCMs~~ of prcp, Tmax and Tmin were examined using the correlation coefficient (R^2) (Eq. (~~7~~8)), Nash-Sutcliff efficiency (NSE) (Eq. (~~8~~9)), and Root mean square error (RMSE) (Eq. (~~9~~10)), [61]. The correlation coefficient (R^2) is a measure of how the ensemble GCMs are likely to be predicted by the model and is equivalent to the sample cross-correlation between ensemble GCMs and observed datasets, where the overbar denotes mean values.

$$R = \frac{\sum_{i=1}^{N_v} (y_i - \bar{y})(o_i - \bar{o})}{\sqrt{\sum_{i=1}^{N_v} (y_i - \bar{y})^2} \sqrt{\sum_{i=1}^{N_v} (o_i - \bar{o})^2}} \quad (\cancel{7}8)$$

where y and o are predicted and observed values, respectively; and N_v is the number of target data used for testing.

The Nash-Sutcliff efficiency (NSE) indicates the goodness-of-fit of the simulated ensemble GCMs and observed data in line 1:1 and can range from −∞ to 1. NSE measures the predictive skill of a model relative to the mean of observations [61]. In this evaluation, the classification suggested by [62] described as: NSE ~~CNS~~ > 0.75 (model is appropriate and good); 0.36 < NSE ~~CNS~~ < 0.75 (model is satisfactory); and NSE ~~CNS~~ < 0.36 (model is unsatisfactory) was adopted.

$$NSE = 1 - \frac{\sum_{i=1}^{n} \left(Y_i^{obs} - Y_i^{sim}\right)^2}{\sum_{i=1}^{n} \left(Y_i^{obs} - Y^{mean}\right)^2} \quad (\cancel{8}9)$$

where Y_i^{obs} is the ith observation for the constituent being evaluated, Y_i^{sim} is the ith simulated value for the constituent being evaluated, Y^{mean} ~~Y_{mean}~~ is the mean of observed data for the constituent being evaluated, and n is the total number of observations.

The Root mean square error (RMSE) measures the global fitness of a predictive model.

$$RMSE = \left(\frac{1}{N} \sum_{i=1}^{N_v} (y_i - o_i)^2 \right)^{1/2} \quad (\cancel{9}10)$$

where y and o are observed and predicted values respectively; and N_v is the number of target data used for testing.

4. Results and discussion

4.1. Ranking of the GCM~~M ensembl~~s~~e~~

Time series GCM and CRU datasets for the period 1980–2005 were used ~~for the~~to calculat~~io~~e~~n~~ ~~of~~the SU weights. The GCMs were then ranked according to the weight derived from the SU technique. The SU weights define the ~~potential~~ advantage of one GCM over the others in simulating the observations. The higher the coefficients, the better performance of the GCM of interest.

The overall scores attained by the GCMs over the entire study area was estimated using equation (4), and the estimated scores for each GCMs are shown in Table 4 respectively. In many cases, small ~~difference in~~ SU weights were~~as~~ observed among the GCMs mainly in ~~precipitation~~ prcp with zero weights in some cases observed in both Tmax and Tmin, which have also been reported in previous studies [17,63]. The smaller difference in SU values among GCMs indicated that all the GCMs performed well with a similar degree of accuracy in replicating observations.

4.2. Spatial distribution of top-ranked GCMs

The SU filter was applied individually to the 26 GCM grid points (0.5°×0.5°) for prcp, Tmax and Tmin with CRU data over the study area. The spatial distribution of the GCM ensemble from the SU filter, which ranks as best, second-best and third-best ~~1st, 2nd and 3rd~~ are shown in figures 2 (a, b & c)~~, represented by different colours based on their SU weights~~. Results obtained shows that ACCESS1.3 was found to be the best GCM in simulating ~~precipitation~~ prcp in the first rank while no single GCM was found to dominate the study areas ~~precipitation~~ prcp in the second and third rank. The spatial distribution of the SU GCMs shows that CSIRO.Mk3L.1.2 was found to dominate the first rank, IPSL.CM45A.LR was also found to dominate the second rank while GFDL.ESM2M was found to dominate the 3rd rank in simulating both Tmax and Tmin GCMs over the entire study area. However, the distribution of SU GCMs shows that MIROC-ESM simulated both Tmax and Tmin in most of the study area.

The Noer.ESM1-M was found to be the best in the western part of the area, while MIROC-ESM was found to be the best in the eastern part of the study area for the Tmax. ACCESS1.3 was also found to dominate the second rank for both, Tmax and Tmin. No single GCM was found to dominate the study areas prcp in the third rank. ~~The Tmin was dominated by MIROC-ESM-CHM~~MIROC-ESM-CHM dominated the Tmin while the CanESM2 was found to perform best in the western part of the area and MIROC.ESM.CHM was found to be the best in the south-eastern part of the area for the Tmax in the third rank.

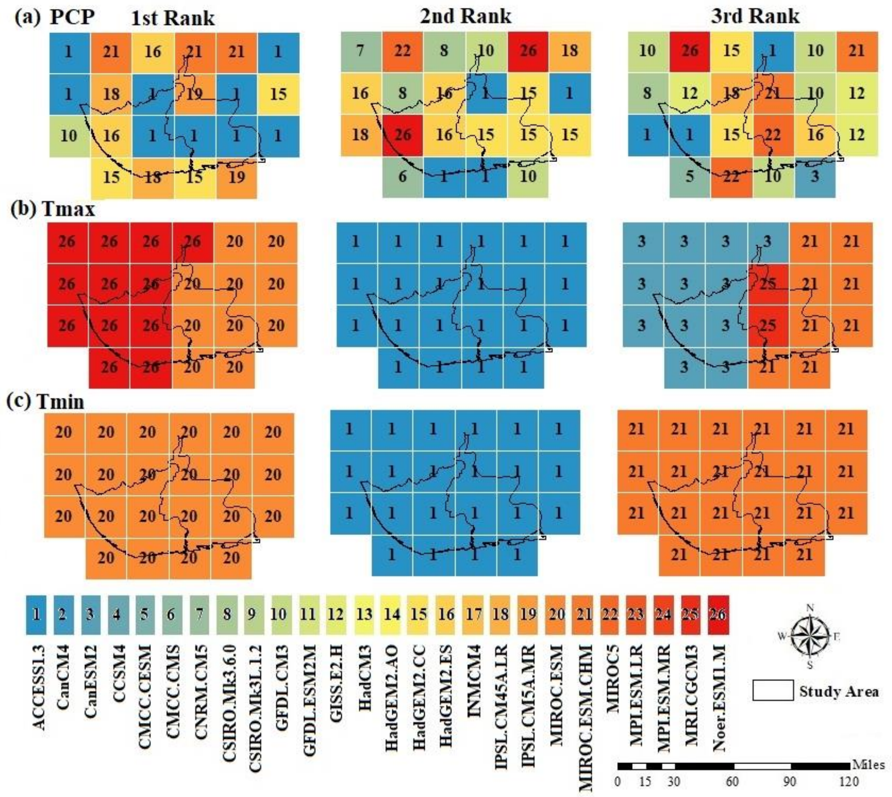

Formatted: Space After: 6 pt

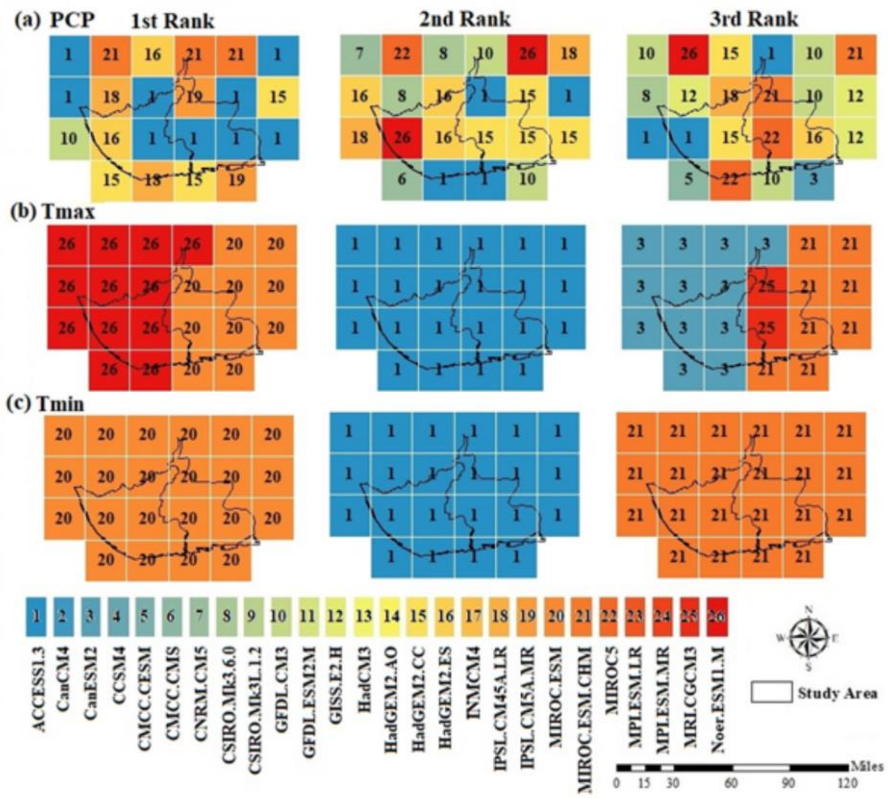

Figure 2. The spatial distribution of GCMs ranked best, second-best and third-best ~~1st, 2nd and 3rd~~ position using symmetrical uncertainty ~~SU~~ filter at different gird points for P~~CP~~rcp, Tmax and Tmin over the Niger Delta.

4.3. Selection of GCM ensemble

GCMs that can simulate both ~~PCP~~Prcp, Tmax and Tmin ~~properly~~ are considered more appropriate ~~desirable~~ for climate change impact analysis [8,19]. ~~Based on these criteria,~~ Twelve GCM outputs shown in bold ranking from the best performing to the worst as summarised in **table 2** met these criteria. ~~t~~The top four GCMs were selected according to their higher SU weight and common performance. **Tables 2** shows the overall GCMs ~~scores~~ ranks~~starting~~ as well as their performances after bias correction in simulating the CRU prcp, Tmax and Tmin obtained from overall weights derived from SU coefficients. The overall scores from the SU filter show that the top four performing GCMs are ACCESS1.3, MIROC-ESM, MIROC-ESM-CHM, and NorESM1-M. These result further verified [16] who suggested that GCMs should be treated independently as separate data points as each model is a myriad of discrete process representations.

Table 2. Overall ~~S~~SU weights of GCMs and their ~~performance~~ ranks according to their ability to simulate CRU prcp, Tmax and Tmin datasets. The selected GCMs are shown in bold fonts.

~~S/no.~~Ranks	GCMs	~~Precipitation~~Prcp			Tmax			Tmin		
		~~Weight~~ SUs	~~NSCN~~ SE	R²	~~Weight~~ SUs	NSE~~C~~	R²	~~Weight~~ SUs	NSE~~C~~	R²

Formatted: Font: Bold
Formatted: Font: 8 pt
Formatted Table
Formatted: Centered
Formatted: Font: 8 pt
Formatted: Font: 8 pt
Formatted: Font: 8 pt
Formatted: Font: 8 pt

1	ACCESS1-3~~ACCESS1.3~~	0.28~~0.208~~	0.58~~0.58~~	0.81~~0.81~~	0.15~~0.094~~	0.67~~0.67~~	0.84~~0.84~~	0.09~~0.090~~	0.86~~-0.86~~	0.55~~0.55~~
2	MIROC-ESM~~CanCM4~~	0.14~~0.007~~	0.63~~0.49~~	0.84~~0.74~~	0.10~~0.008~~	0.87~~0.91~~	0.44~~0.91~~	0.12~~0.008~~	0.62~~0.65~~	0.49~~0.48~~
3	MIROC-ESM-CHM~~CanESM2~~	0.15~~0.022~~	0.69~~0.52~~	0.56~~0.77~~	0.11~~0.015~~	0.86~~-2.18~~	0.86~~0.67~~	0.02~~0.012~~	0.50~~-6.48~~	0.58~~0.25~~
4	Noer-ESM1-M~~CCSM4~~	0.13~~0.099~~	0.57~~0.51~~	0.82~~0.76~~	0.14~~0~~	0.82~~-0.70~~	0.89~~0.66~~	0.05~~0~~	0.38~~0.44~~	0.48~~0.46~~
5	MIROC5~~CMCC.CESM~~	0.08~~0.019~~	0.62~~0.61~~	0.82~~0.81~~	0.15~~0~~	-5.36~~0.89~~	0.88~~0.89~~	0.06~~0~~	-1.88~~0.65~~	0.45~~0.48~~
6	HadGEM2-ES~~CMCC.CMS~~	0.19~~0.004~~	0.59~~0.55~~	0.81~~0.78~~	0.03~~0.042~~	0.88~~0.63~~	0.91~~0.79~~	0.02~~0.042~~	0.54~~0.31~~	0.53~~0.45~~
7	CanCM4~~CNRM.CM5~~	0.07~~0.046~~	0.49~~0.44~~	0.74~~0.73~~	0.08~~0.010~~	0.91~~0.64~~	0.91~~0.81~~	0.01~~0.010~~	0.65~~0.28~~	0.48~~0.51~~
8	MRI-CGCM3~~CSIRO.Mk3.6.0~~	0.06~~0.043~~	0.55~~0.44~~	0.78~~0.71~~	0.11~~0~~	0.70~~0.15~~	0.87~~0.83~~	0.03~~0~~	0.48~~-0.06~~	0.51~~0.57~~
9	MPI-ESM-MR~~CSIRO.Mk3L.1.2~~	0.06~~0.040~~	0.35~~0.31~~	0.78~~0.60~~	0.05~~0~~	0.75~~0.89~~	0.87~~0.89~~	0.02~~0~~	0.49~~0.68~~	0.51~~0.53~~
10	CMCC-CMS~~GFDL.CM3~~	0.08~~0.162~~	0.55~~-0.35~~	0.78~~0.42~~	0.11~~0~~	0.63~~-0.62~~	0.79~~0.15~~	0.04~~0~~	0.31~~0.37~~	0.45~~0.20~~
11	CNRM-CM5~~GFDL.ESM2M~~	0.10~~0.175~~	0.44~~0.49~~	0.73~~0.74~~	0.07~~0~~	0.64~~0.79~~	0.81~~0.85~~	0.01~~0~~	0.28~~0.40~~	0.51~~0.55~~
12	CanESM2~~GISS.E2.H~~	0.10~~0.066~~	0.52~~0.32~~	0.77~~0.62~~	0.12~~0~~	-2.18~~0.74~~	0.67~~0.76~~	0.01~~0~~	-6.48~~0.56~~	0.25~~0.37~~
13	IPSL-CM45A-LR~~HadCM3~~	0.15~~0.138~~	0.63~~0.58~~	0.85~~0.80~~	0.03~~0~~	0.81~~0.91~~	0.91~~0.91~~	0~~0~~	0.42~~0.67~~	0.57~~0.51~~
14	HadGEM2-CC~~HadGEM2.AO~~	0.21~~0.138~~	0.58~~0.62~~	0.82~~0.83~~	0~~0~~	0.90~~0.84~~	0.90~~0.81~~	0~~0~~	0.63~~0.49~~	0.45~~0.29~~
15	HadCM3~~HadGEM2.CC~~	0.09~~0.001~~	0.58~~0.58~~	0.80~~0.82~~	0~~0.003~~	0.91~~0.90~~	0.91~~0.90~~	0~~0.004~~	0.67~~0.63~~	0.51~~0.45~~
16	CMCC-CESM~~HadGEM2.ES~~	0.08~~0.154~~	0.61~~0.59~~	0.81~~0.81~~	0.00~~0.022~~	0.89~~0.88~~	0.89~~0.91~~	0~~0.019~~	0.65~~0.54~~	0.48~~0.53~~
17	IPSL-CM5A-MR~~INMCM4~~	0.11~~0.013~~	0.47~~0.42~~	0.74~~0.68~~	0~~0~~	0.84~~0.60~~	0.85~~0.69~~	0~~0~~	0.64~~-0.54~~	0.46~~0.42~~

18	GFDL-ESM2M~~IPSL.CM45A.LR~~	0.11~~0.133~~	0.49~~0.63~~	0.74~~0.85~~	0.04~~0~~	0.79~~0.81~~	0.85~~0.91~~	0~~0~~	0.40~~0.42~~	0.55~~0.57~~
19	CSIRO-Mk3L-1-2~~IPSL.CM5A.MR~~	0.05~~0.004~~	0.31~~0.47~~	0.60~~0.74~~	0~~0~~	0.89~~0.84~~	0.89~~0.85~~	0~~0~~	0.68~~0.64~~	0.53~~0.46~~
20	HadGEM2-AO~~MIROC.ESM~~	0.03~~0.281~~	0.62~~0.62~~	0.83~~0.82~~	0~~0.122~~	0.84~~0.87~~	0.81~~0.88~~	0~~0.121~~	0.49~~0.62~~	0.29~~0.45~~
21	GISS-E2-H~~MIROC.ESM.CHM~~	0.14~~0.199~~	0.32~~0.63~~	0.62~~0.84~~	0~~0.024~~	0.74~~-5.36~~	0.76~~0.44~~	0~~0.056~~	0.56~~-1.88~~	0.37~~0.49~~
22	MPI-ESM-LR~~MIROC5~~	0.06~~0.005~~	0.55~~0.69~~	0.80~~0.56~~	0~~0~~	0.00~~0.86~~	0.87~~0.86~~	0~~0.025~~	0.63~~0.50~~	0.56~~0.58~~
23	CSIRO-Mk3-6-0~~MPI.ESM.LR~~	0.13~~0.004~~	0.44~~0.55~~	0.71~~0.80~~	0.02~~0.016~~	0.15~~0.00~~	0.83~~0.87~~	0~~0~~	-0.06~~0.63~~	0.57~~0.56~~
24	INMCM4~~MPI.ESM.MR~~	0.05~~0.004~~	0.42~~0.35~~	0.68~~0.78~~	0~~0.034~~	0.60~~0.75~~	0.69~~0.87~~	0~~0.017~~	-0.54~~0.49~~	0.42~~0.51~~
25	CCSM4~~MRI.CGCM3~~	0.09~~0.023~~	0.51~~0.55~~	0.76~~0.78~~	0~~0.055~~	-0.70~~0.70~~	0.66~~0.87~~	0~~0.033~~	0.44~~0.48~~	0.46~~0.51~~
26	GFDL-CM3~~Noer.ESM1.M~~	0.21~~0.018~~	-0.35~~0.57~~	0.42~~0.82~~	0~~0.046~~	-0.62~~0.82~~	0.15~~0.89~~	0~~0.047~~	0.37~~0.38~~	0.20~~0.48~~

4.4. Ensemble model validation

The performance of the ensemble model at each grid point, for all the 26 GCMs, 4 SU selected GCMs and CRU datasets were assessed by the coefficient of correlation (R^2) and Nash-Sutcliff efficiency (NSE). As an example, results obtained from the grid point in Port Harcourt is presented in Table 3, respectively. The results indicated that the ranking of GCMs assisted in identifying a better-performing GCM ensemble for downscaling of simulations/ projections and can be a possible way to produce more reliable hydro-climatic information at a finer spatial resolution and with reduced uncertainties.

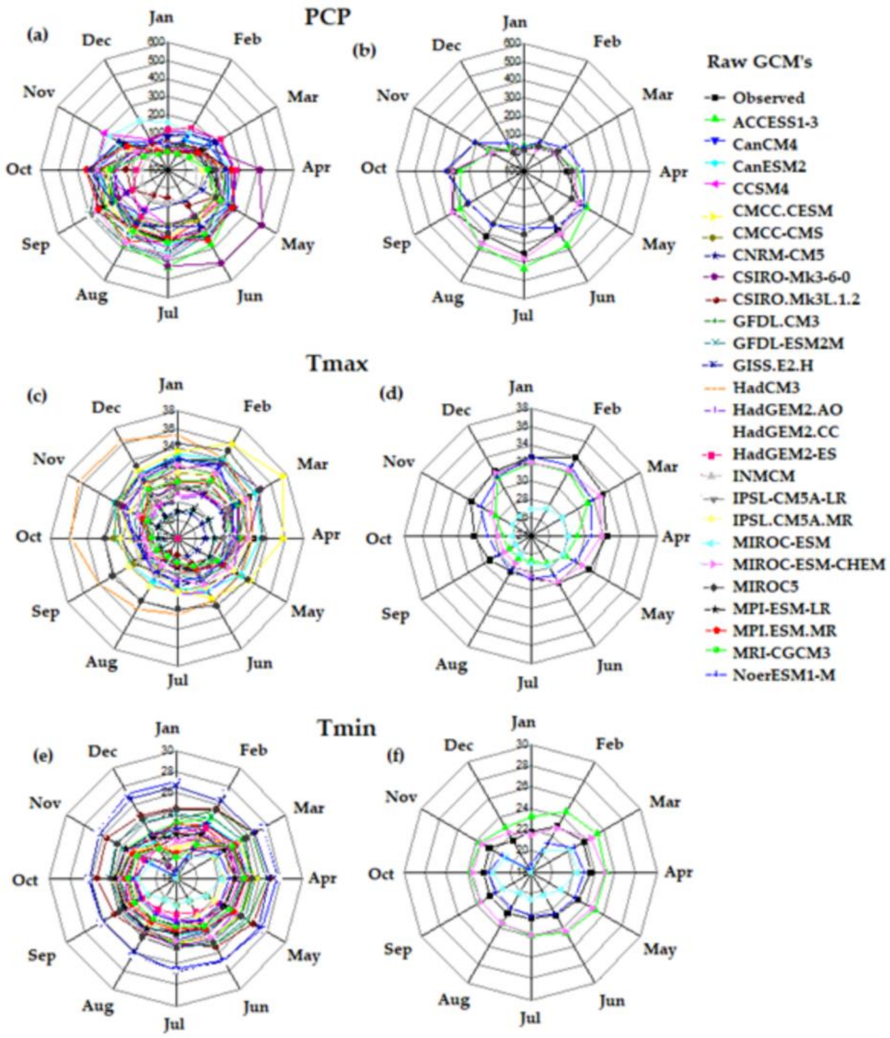

Figure 3. Monthly averages of CRU and Raw datasets (a) 26 Prcp (b) 4 Prcp SU (c) 26 Tmax (d) 4 Tmax SU (e) 26 Tmin (f) 4 Tmin SU GCM outputs for the Historical periods 1980 – 2005 at the grid point located in Port Harcourt.

~~(a) 26 PCP GCMs (b) 4 PCP SU GCMs (c) 26 Tmax GCMs (d) 4 Tmax SU GCMs (e) 26 Tmin GCMs (f) 4 Tmin SU GCMs for the Historical periods 1980 – 2005 at the grid located in Port Harcourt.~~

Formatted: Right: 0 cm

Comparative plots of mean monthly raw 26 GCMs and the 4 SU selected GCMs shown in figure 3 shows that the selected GCM outputs match~~es~~ better with the observed CRU datasets which suggested a better performance after bias correction as clearly proved by figures 4 respectively. Results of comparative analysis between the ensemble of all GCMs and the ensemble SU selected GCMs over the ~~selected~~ grid points ~~and~~ as depicted in Table 3 showed low RMSE with high ~~NSC~~ NSE and R^2 values which shows that the SU ensemble performs better in depicting the CRU datasets. The ensemble of all GCMs ~~consistently~~ underestimated the sum (2166.91 mm) and the mean (5.94 mm) of CRU prcp (2227.95 mm & 6.19 mm), respectively. However, application

Formatted: Indent: First line: 0.74 cm, Right: 0 cm, Space Before: 0 pt, After: 0 pt of the SU filter in ensemble selection improved the results to a sum of 2255.49 mm and a mean of 6.23 mm. This trend was observed in all the 22 grid points. Comparison of the mean values obtained at all the grid points for Tmax and Tmin confirms the better performances of the SU model.

The seasonal averages of the ~~bias-~~bias-corrected 26 GCM output ~~s~~and the four selected models were compared to that of the CRU datasets in order to assess the performance of the downscaled model presented in figure 4 below. The figures show that the selected GCMs matched better with the CRU datasets after correcting the biases which~~–~~ are assumed to indicate that they produce more realistic projections.~~shows is an indicator that they will produce a better ensemble.~~

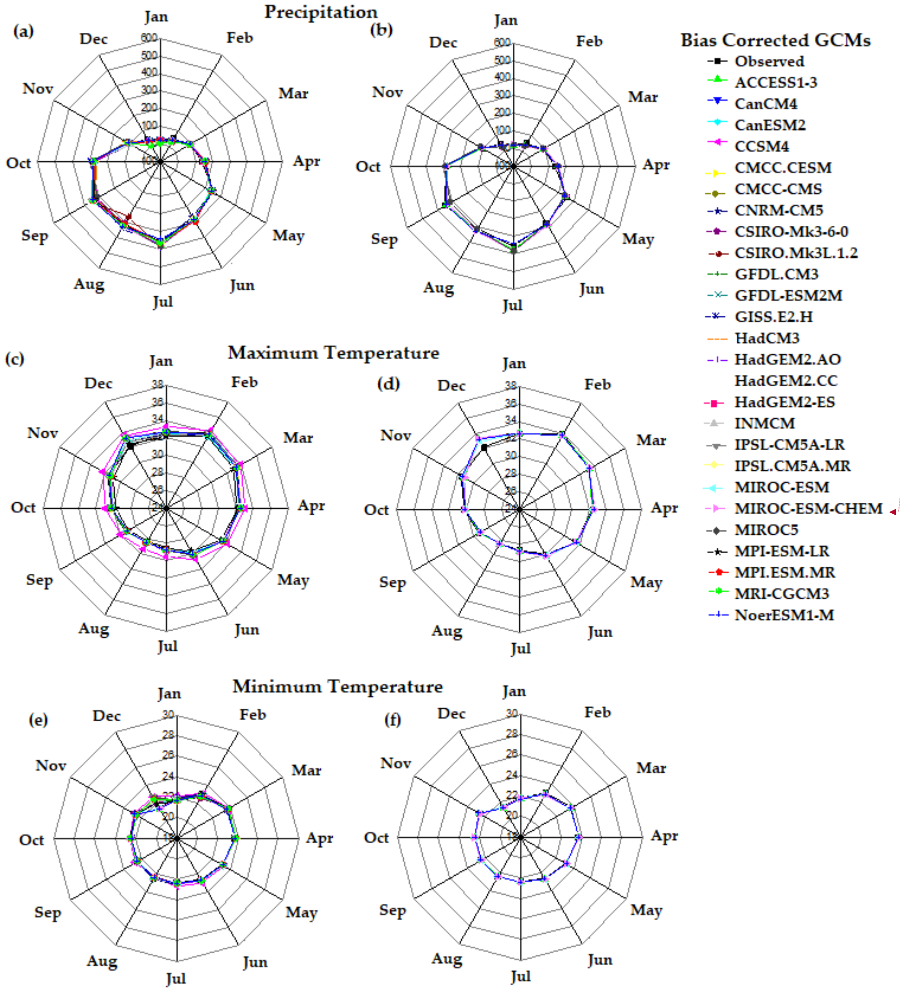

432

Formatted: Space Before: 0 pt

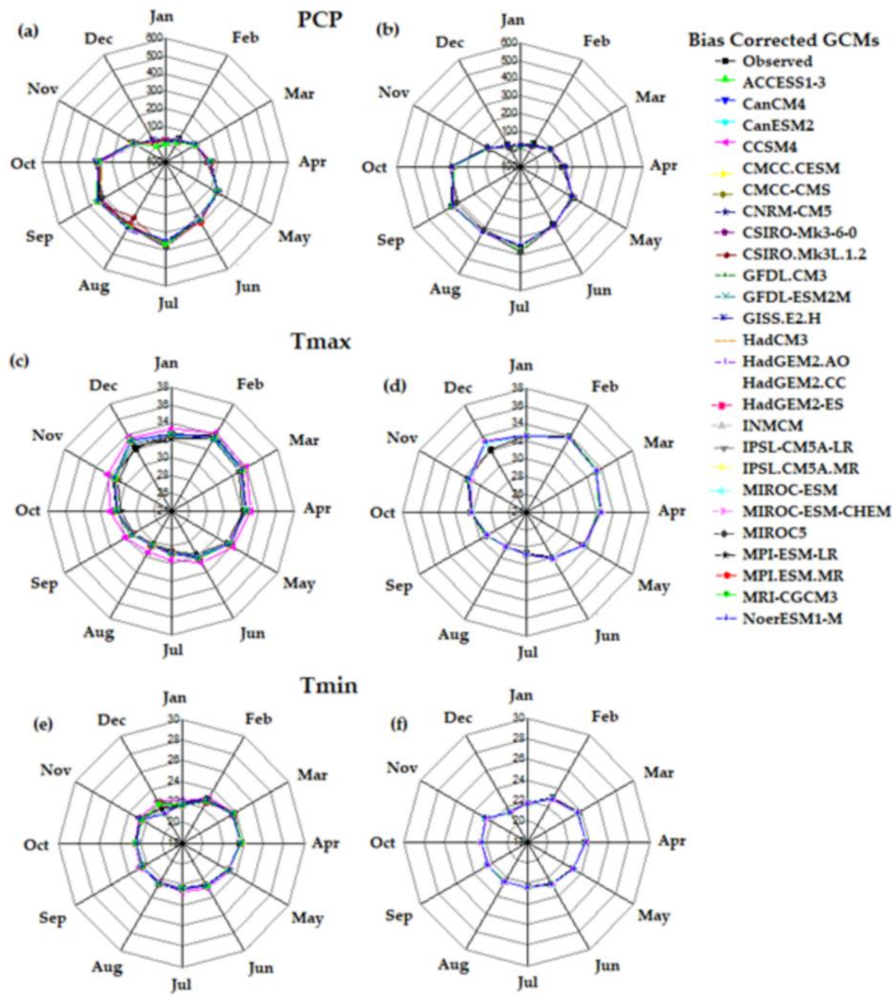

Figure 4. Monthly averages of CRU and Bias corrected datasets (a) 26 P~~CP~~rcp ~~GCMs~~ (b) 4 ~~PCP~~ Prcp SU ~~GCMs~~ (c) 26 Tmax ~~GCMs~~ (d) 4 Tmax SU ~~GCMs~~ (e) 26 Tmin ~~GCMs~~ (f) 4 Tmin SU GCM outputs for the Historical periods 1980 – 2005 at the grid -point located in Port Harcourt.

The obtained results were further validated using interval plots of changes in the annual averages of CRU datasets with the ensemble of all the 26 GCMs and the 4 selected SU GCMs for prcp, Tmax and Tmin (Figure 5). The changes and the levels of uncertainty were estimated using the RMSE and 95% confidence band shows the spread of the uncertainties during the future periods. ~~The obtained results were further validated using the plots of monthly averages of CRU datasets with the ensembles of all the 26 GCMs, SU selected ensemble as depicted in figure 5. Most of the data were found to align with the CRU observations for both pcp, Tmax and Tmin. However, a slight variation can also be seen. The variation is relatively higher during December for Tmax and Tmin and typical for All and SU ensemble.~~ The results obtained~~These~~ indicated the efficiency of the SU ensemble models in GCM selection. Overall, the SU filter was found to perform well in improving GCM~~s~~

ensemble selection for simulating the sum and mean~~, low, and extreme~~ values in the region, as shown in table 3.

Table 3. Performance assessment of GCM ensemble~~s~~ at the grid located in Port Harcourt.

Mean Annual		Observed	GCM Ensemble~~s~~	
			All	**SU**
~~**Precipitation**~~ **Prcp (mm)**	**Sum**	2227.95	2166.91	2255.49
	Mean	6.19	5.94	6.23
	RMSE	-	2.42	2.62
	~~**NSC**~~**NSE**	-	0.58	0.62
	R^2	-	0.86	0.83
Tmax (°C)	**Mean**	31.13	31.20	31.06
	RMSE	-	0.68	0.71
	~~**NSC**~~**NSE**	-	1.00	1.00
	R^2	-	0.92	0.92
Tmin (°C)	**Mean**	22.63	23.12	22.72
	RMSE	-	0.88	1.17
	~~**NSC**~~**NSE**	-	1.00	1.00
	R^2	-	0.64	0.62

~~The results showed proper matching of SU ensemble mean Pcp, Tmax and Tmin with CRU. Thus, the results indicate that the SU ensemble selection approach can improve the accuracy in the projection by reducing uncertainties associated with individual GCMs.~~

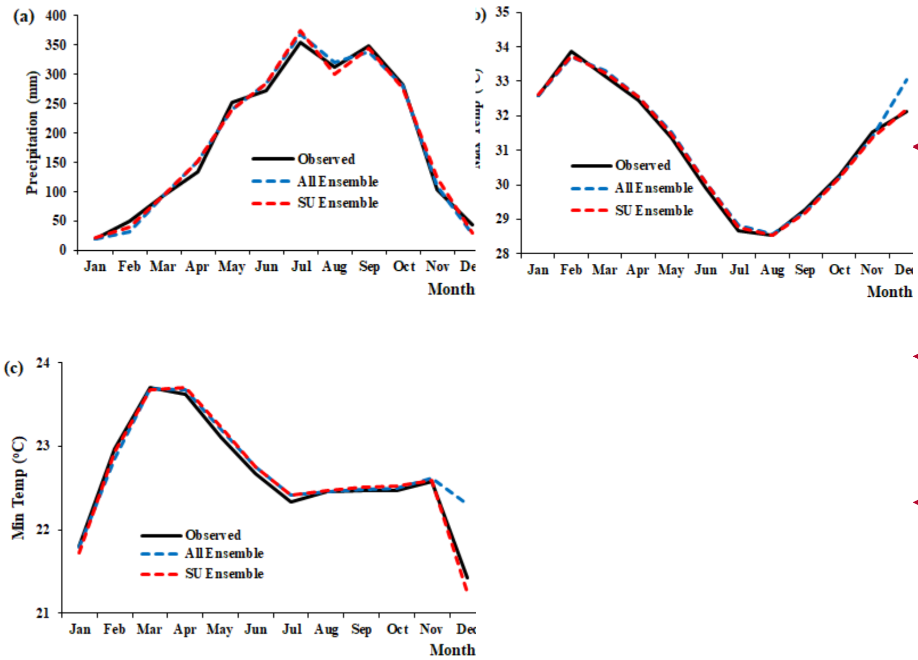

Formatted: Space Before: 6 pt

Formatted: Space Before: 0 pt

Formatted: Indent: Left: 0 cm, Space Before: 12 pt

Formatted Table

Formatted: Right: -0.51 cm, Space Before: 12 pt

Formatted: Space Before: 12 pt

Formatted: MDPI_5.1_figure_caption, Left, Indent: Left: 0.51 cm, Right: 0.51 cm, Automatically adjust right indent when grid is defined, Space Before: 12 pt

Formatted: Left, Indent: Left: 0 cm, Right: 0 cm

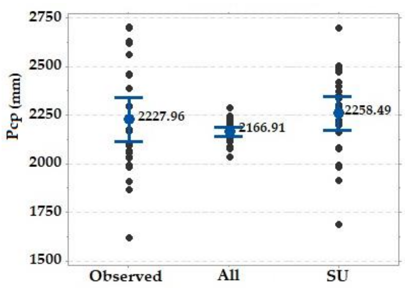

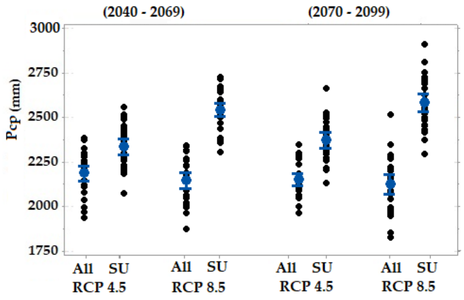

(a) (b)

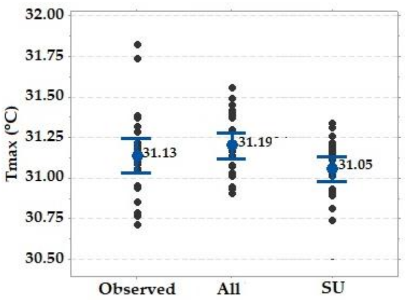

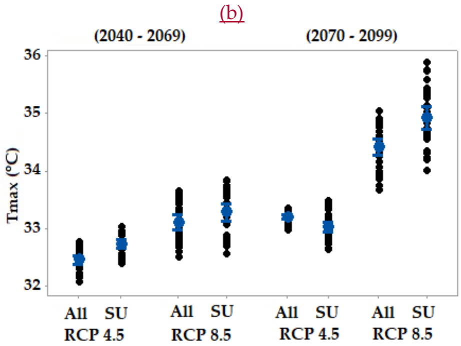

(c) (d)

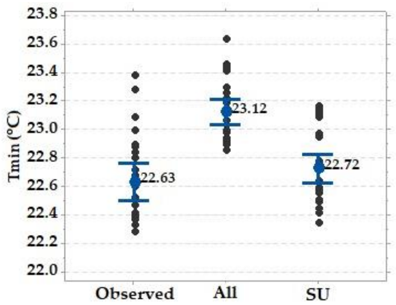

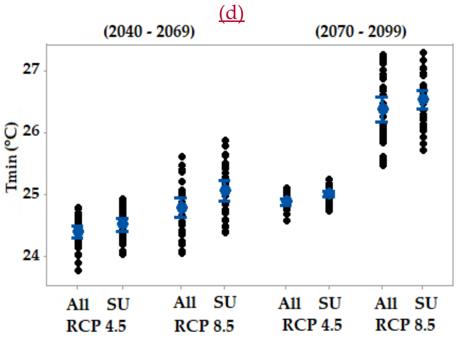

(e) (d)

Figure 5. Interval plots for the annual averages of CRU datasets with the ensemble of all the 26 GCMs and the 4 SU selected GCMs for (a) Prcp (Base Periods) (b) Prcp (future Periods) (c) Tmax (Base Periods) (d) Tmax (future Periods) (e) Tmin (Base Periods) (f) Tmin (future Periods) with 95% confidence interval at the grid located in Port Harcourt.

~~**Figure 5.** Monthly averages of CRU datasets with the ensembles of all the 26 GCMs and the selected SU GCMs for (a) Precipitation (b) Tmax (c) Tmin at the grid located in Port Harcourt.~~The results showed a reproduction of CRU observed datasets by the SU ensemble mean for Prcp, Tmax and Tmin. Thus, indicate that the SU ensemble selection approach can improve the accuracy in the projection by reducing uncertainties associated with individual GCMs.

4.5. Spatial changes in mean annual ~~precipitation~~Prcp, Tmax and Tmin

Formatted: Space Before: 6 pt

Formatted Table

Formatted: Space Before: 6 pt

Formatted: Space Before: 6 pt

Formatted: Indent: Left: 0 cm, Right: 0 cm

Formatted: Font: Not Bold

Formatted: Font: Not Bold

Formatted: Indent: Left: 0 cm, First line: 0.74 cm, Right: 0 cm, Space Before: 0 pt

The SU selected GCM~~s~~ ensemble was used in this study to map the generated mean changes in Prcp, Tmax and Tmin in the Niger Delta. To estimate these percentage changes, the averages of the CRU prcp, Tmax and Tmin for the base period 1980–2005 at all grid points were subtracted from those of the projected prcp, Tmax and Tmin for the different future periods, 2040–2069, and 2070–2099 as~~The percentage changes in annual precipitation for periods 2040–2069 and 2070–2099 were estimated considering 1980–2005 as the base period. The spatial patterns of precipitation changes under RCP4.5 and RCP8.5 scenarios from 2040–2069 and from 2070–2099 is~~ shown in figures 6, 7 and 8 respectively.

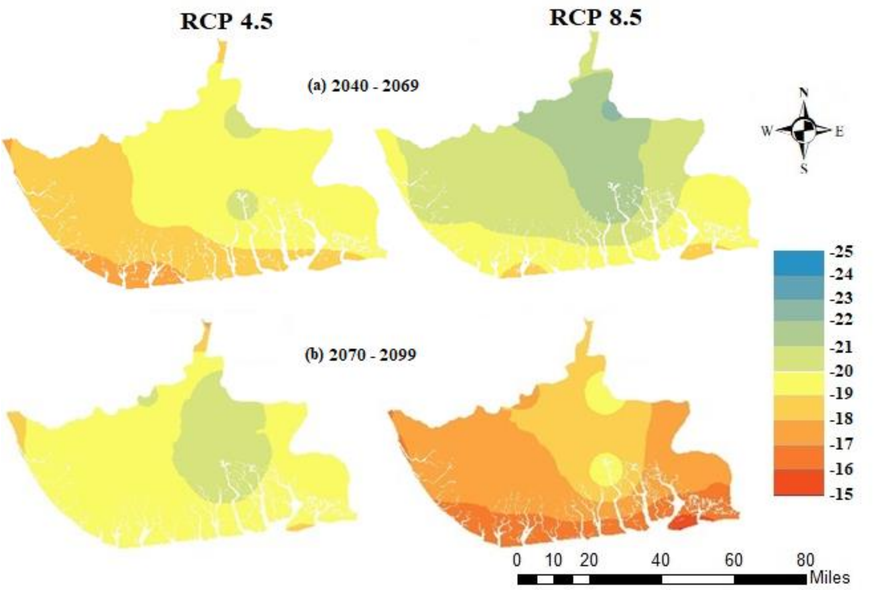

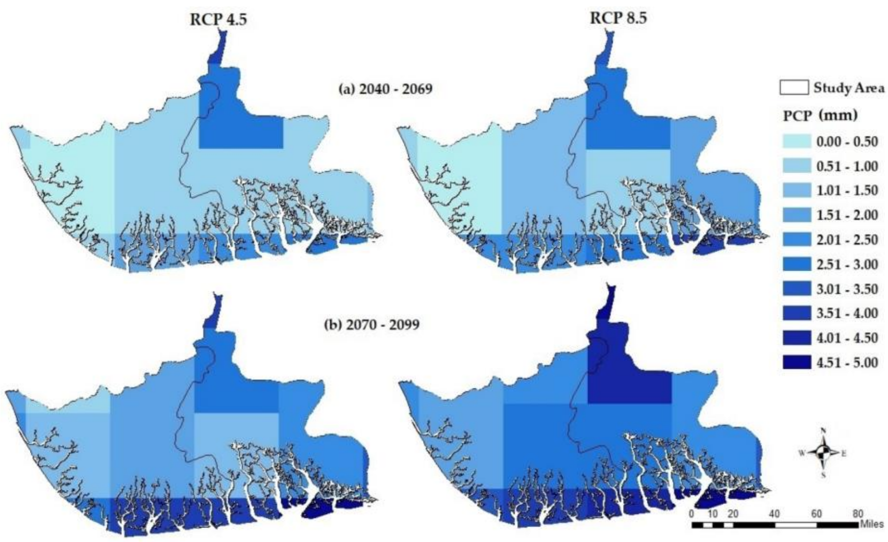

Formatted: Space After: 6 pt

Figure 6. Spatial distribution of percentage changes in average ~~average~~ annual ~~precipitation~~prcp, for periods (a) 2040–2069 (b) 2070–2099~~)~~ compared to the base period 1980–2005 for ~~the two scenarios namely,~~ RCP4.5 and RCP8.5.

Formatted: Indent: Left: 0.51 cm, Right: 0.25 cm

~~A decrease in precipitation in the range of -25 to -15% was noticed over a considerable area. However, most of the decrease in precipitation was noticed mainly over some parts in the east, while a small area around the coast showed a lesser decrease in precipitation. The spatial patterns of precipitation change are found to decrease over a larger area during 2070–2099 compared to 2040–2069 under RCP 4.5 while the percentage precipitation change was found to decrease more during 2040–2069 compared to 2070–2099 under RCP 8.5. The figures show that the mean annual precipitation in the Niger Delta decreased significantly between the range of 19–23% under RCP4.5 and 13-19% under RCP8.5 across the study area for all future periods. The finding of present study collaborates with that obtained by [19]. This pattern of decrease in precipitation is also being observed by [62] at the global scale.~~

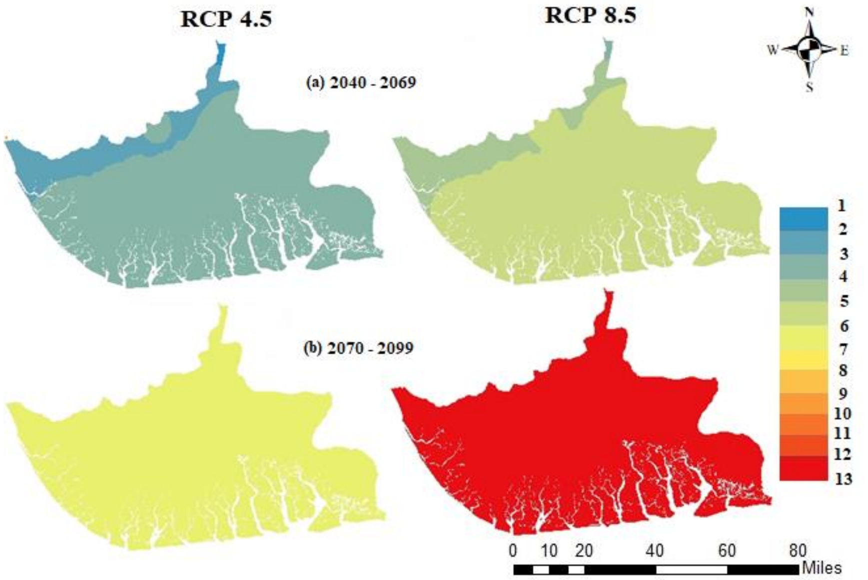

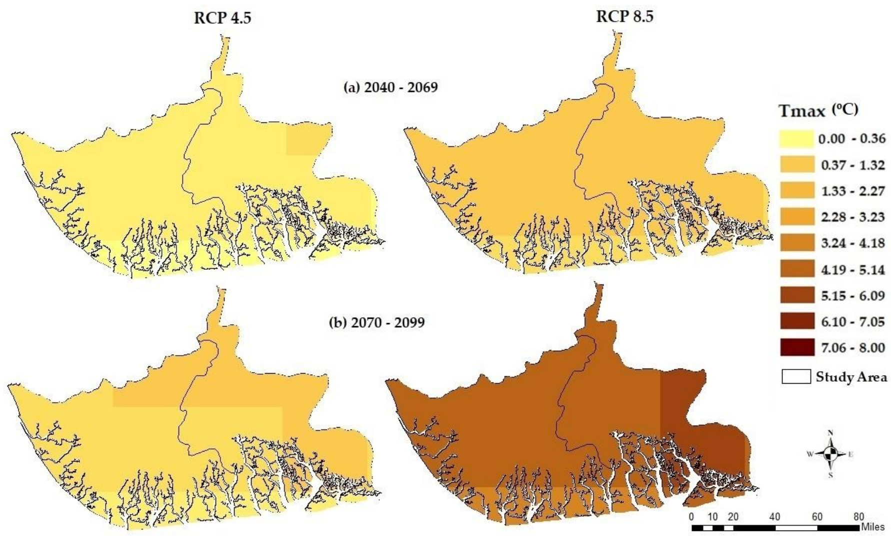

Figure 7. Spatial distribution of percentage changes in average annual Maximum Temperature, for periods (a) 2040–2069 (b) 2070–2099 compared to the base period 1980–2005 for ~~the two scenarios namely,~~ RCP4.5 and RCP8.5.

Formatted: Space Before: 0 pt, After: 0 pt

Formatted: Space Before: 0 pt

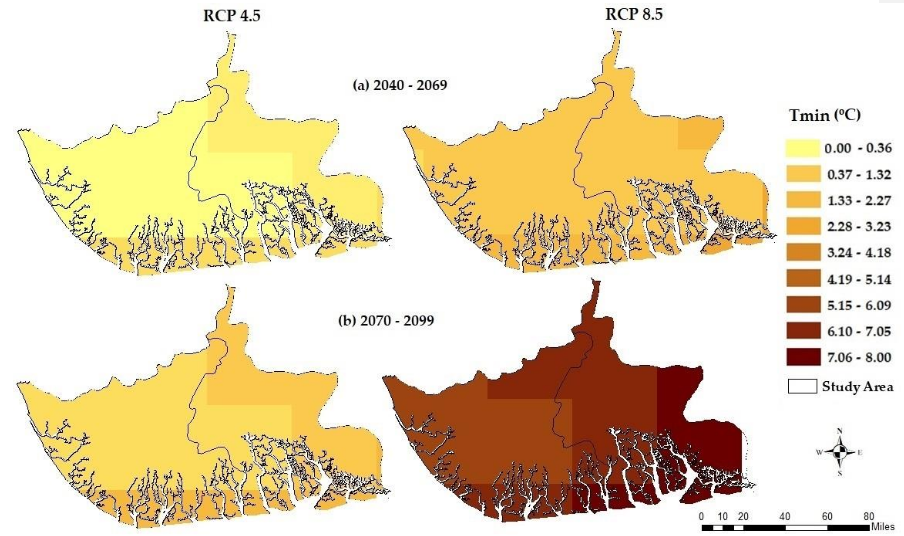

~~The spatial distribution of the percentage changes in projections of Tmax and Tmin during the last part of this century (2070–2099) based on selected RCP scenarios (RCP4.5 and RCP8.5) are shown in Figure 7 and 8 respectively. However, the projected changes in annual Tmax and Tmin shows an increasing trend across the study area for all future periods and all the RCPs. Tmax is projected to increase significantly by 3–8% (0.9–1.95 °C) under RCP4.5 and between 11–12% (3.6–3.8 °C) under RCP8.5 during the periods 2070–2099. Tmin is also expected to increase significantly by 9–10% (2.25 °C) under RCP4.5 and between 16–17% (3.6–3.8 °C) under RCP8.5 during the periods 2070–2099. This behaviour has also been observed and modelled in other parts of the world [63–66].~~

~~Though a number of studies have been conducted to assess future changes in pcp, Tmax and Tmin at global scales, only limited studies have been conducted in west Africa and Nigeria at large. The present study is entirely different from all the previous studies in term of projection of both precipitation and temperature using a SU ensemble of systematically selected GCMs. [19] assessed the future changes and selection of suitable sets of precipitation in Nigeria for all the future periods and all emission scenarios.~~

~~This is the first attempt for selection of a suitable set of daily GCMs based on their capability to simulate both precipitation and temperature together for the spatiotemporal projection changes in the Niger Delta. Therefore, it is expected that the results obtained in this study will help in impact assessment and adaptation studies in Niger Delta at local scale as the projection of rainfall along with temperature is highly essential for climate change impact assessment.~~

Formatted: Space After: 12 pt

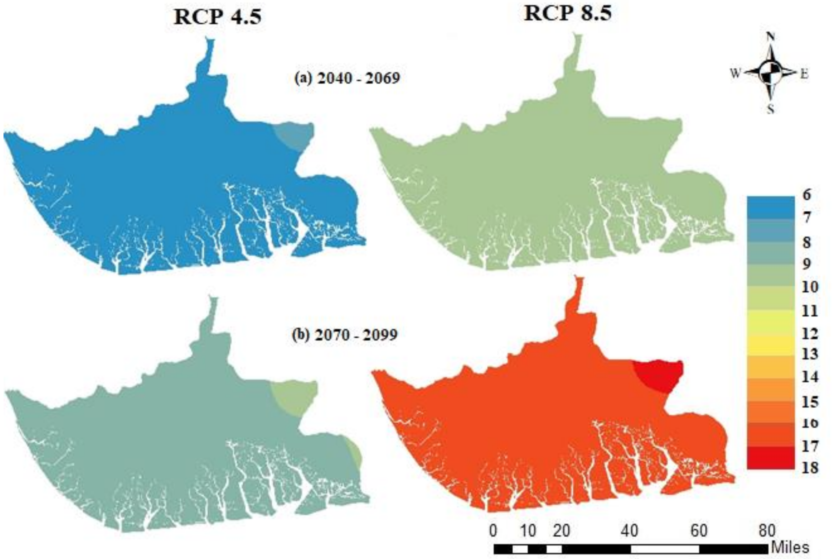

Figure 8. Spatial distribution of percentage changes in average annual Minimum Temperature, for periods (a) 2040–2069 (b) 2070–2099 compared to the base period 1980–2005 for ~~the two scenarios namely,~~ RCP4.5 and RCP8.5.

Figure 6 shows the variation in pcp changes across the area. The coastal areas are generally projected to have the highest percentage of changes in pcp for all RCPs and future periods while the north-western part showed the lowest percentage changes. The changes in pcp range between 0.3% to 3.78% under RCP 4.5, and 1.62% to 4.74% under RCP 8.5 for the period, 2040–2069. During the period 2070–2099, a change between 0.26% to 3.57% under RCP 4.5, and 0.7% to 4.94% under RCP 8.5 was also projected across the study area.

The projected changes in annual Tmax and Tmin (Figures 7 and 8) shows an increasing trend across the study area for both future periods and RCPs. Tmax is projected to increase significantly by 3-8% (0.4 °C) under RCP4.5 and between 3.89-5.47% (1.25-1.79 °C) under RCP8.5 during the periods 2070–2099. Tmin is also expected to increase significantly by 0.31-2.52% (0.52 °C) under RCP4.5 and between 5.64-8.22% (1.38-2.02 °C) under RCP8.5 during the periods 2070–2099 as expected in response to greenhouse gasses forcing which is consistent with other parts of the world [64–67].

Formatted: Indent: Left: 0 cm, First line: 0.74 cm, Right: 0 cm, Space Before: 0 pt, After: 0 pt

Based on the projected values of simulated climatic variables over the study area, the projected increase of this climate variable confirms the report of IPCC, [1] as well as [37,68–70] in this region. These increase will further aggravate the vulnerability of the water quality, water resources, agricultural land, fisheries and livestock in the Niger Delta coastal zone to climate change. The region might experience more extreme floods which might threaten the livelihood and socio-economic growth of the region which might also have a significant impact on Nigeria's GDP as the primary sources of the country's revenue is the oil and gas from the study area.

5. Conclusions

A suitable set of GCM ensemble for simulating the Spatio-temporal changes in both prcp, Tmin and Tmax were selected based on their performances in simulating the observed CRU datasets using the symmetrical uncertainty (SU) filter using 26 GCM outputs, under RCP4.5 and RCP8.5 emission scenarios. The study identified four GCMs, namely ACCESS1.3, MIROC-ESM, MIROC-ESM-CHM, and NorESM1-M as the most suitable set of GCMs for simulating both prcp, Tmax and Tmin over the

Formatted: Justified, Indent: First line: 0.74 cm, Space After: 0 pt

Niger Delta. Though several studies have been conducted to assess future changes in prcp, Tmax and Tmin at global scales, only limited studies conducted in West Africa and Nigeria. This study, therefore, the first attempt to employ a selection of a suitable set of daily GCMs to simulate both prcp, Tmin and Tmax together for the spatiotemporal projection changes in the Niger Delta.

The findings of this study predicted an increase in both Tmin, Tmax and prcp for both periods and RCPs. The predicted increase in future pcp and temperature is useful to inform all the stakeholders of the need to regulate anthropogenic activities such as gas flaring, illegal refining of crude oil and other petrochemical products which release more CO_2 and other greenhouse gases into the atmosphere in this region. This study will be useful in sustainable environmental management in the extreme weather driven by emerging climate change in the coastal zones of the Niger Delta, Nigeria.

~~The objective of this study was to select the suitable set of GCM ensemble for simulating both precipitation and temperature together for spatiotemporal projection of changes in the Niger Delta. The GCMs are selected using state-of-art feature selection method namely SU for better performance. Twenty-six CMIP5 GCMs which have both precipitation and temperature projections with 2 RCP scenarios (RCP4.5 and RCP8.5) for Nigeria were used for selection of GCMs ensemble for the Niger Delta. The study identified four GCMs namely ACCESS1.3, MIROC-ESM, MIROC-ESM-CHM, and NorESM1-M as most suitable for projection of both pcp, Tmax and Tmin over the Niger Delta. The study revealed a decrease in precipitation across the area and an increase in both Tmax and Tmin. These findings collaborate very well with findings in most of the world that shows Tmin will increase more compared to Tmax and the precipitation decrease in coastal areas across the globe. The gridded datasets and GCMs are selected in this study solely based on their performances in simulating the CRU precipitation and temperature datasets.~~

Author Contributions: Funding: This research was funded by the Petroleum Technology and Development Fund (PTDF) under the Overseas PhD scholarship scheme and supported by the Scottish Government under the Climate Justice Fund Water Futures Programme, awarded to the University of Strathclyde (R.M. Kalin).

Conflicts of Interest: The authors declare no conflict of interest.

References~~:~~

1. IPCC. *Climate Change 2007: Impacts, Adaptation and Vulnerability: Contribution of Working Group II to the Fourth Assessment Report of the Intergovernmental Panel*; 2007. https://doi.org/10.1256/004316502320517344.
2. Northrop, P. J. A Simple, Coherent Framework for Partitioning Uncertainty in Climate Predictions". *J. Clim.* **2013**, *26* (12), 4375–4376. https://doi.org/10.1175/JCLI-D-12-00527.1.
3. Ahmed, K.; Shahid, S.; Wang, X.; Nawaz, N.; Najeebullah, K. Evaluation of Gridded Precipitation Datasets over Arid Regions of Pakistan. *Water (Switzerland)* **2019**, *11* (2). https://doi.org/10.3390/w11020210.
4. Sun, Q.; Miao, C.; Duan, Q.; Ashouri, H.; Sorooshian, S.; Hsu, K. L. A Review of Global Precipitation Data Sets: Data Sources, Estimation, and Intercomparisons. *Rev. Geophys.* **2018**, *56* (1), 79–107. https://doi.org/10.1002/2017RG000574.
5. Hijmans, R. J.; Cameron, S. E.; Parra, J. L.; Jones, P. G.; Jarvis, A. Very High Resolution Interpolated Climate Surfaces for Global Land Areas. *Int. J. Climatol.* **2005**, *25* (15), 1965–1978. https://doi.org/10.1002/joc.1276.
6. Khan, N.; Shahid, S.; Ahmed, K.; Ismail, T.; Nawaz, N.; Son, M. Performance Assessment of General Circulation Model in Simulating Daily Precipitation and Temperature Using Multiple Gridded Datasets. *Water (Switzerland)* **2018**, *10* (12). https://doi.org/10.3390/w10121793.
7. IPCC. Climate Change The IPCC Scientific Assessment. *Ipcc*. 1990, p 414. https://doi.org/10.1097/MOP.0b013e3283444c89.

Formatted: Justified, Indent: First line: 0.74 cm, Space Before: 0 pt, After: 0 pt

Formatted: Subscript

Formatted: Font color: Red

8. Salman, S. A.; Shahid, S.; Ismail, T.; Ahmed, K.; Wang, X. J. Selection of Climate Models for Projection of Spatiotemporal Changes in Temperature of Iraq with Uncertainties. *Atmos. Res.* **2018**, *213* (July), 509–522. https://doi.org/10.1016/j.atmosres.2018.07.008.
9. Chen, J.; Brissette, F. P.; Leconte, R. Uncertainty of Downscaling Method in Quantifying the Impact of Climate Change on Hydrology. *J. Hydrol.* **2011**, *401* (3–4), 190–202. https://doi.org/10.1016/j.jhydrol.2011.02.020.
10. Foley, A. M. Uncertainty in Regional Climate Modelling: A Review. *Prog. Phys. Geogr.* **2010**, *34* (5), 647–670. https://doi.org/10.1177/0309133310375654.
11. Lutz, A. F.; ter Maat, H. W.; Biemans, H.; Shrestha, A. B.; Wester, P.; Immerzeel, W. W. Selecting Representative Climate Models for Climate Change Impact Studies: An Advanced Envelope-Based Selection Approach. *Int. J. Climatol.* **2016**, *36* (12), 3988–4005. https://doi.org/10.1002/joc.4608.
12. Ahmed, K.; Shahid, S.; Sachindra, D. A.; Nawaz, N.; Chung, E. S. Fidelity Assessment of General Circulation Model Simulated Precipitation and Temperature over Pakistan Using a Feature Selection Method. *J. Hydrol.* **2019**, *573* (November 2018), 281–298. https://doi.org/10.1016/j.jhydrol.2019.03.092.
13. Lin, C. Y.; Tung, C. P. Procedure for Selecting GCM Datasets for Climate Risk Assessment. *Terr. Atmos. Ocean. Sci.* **2017**, *28* (1), 43–55. https://doi.org/10.3319/TAO.2016.06.14.01(CCA).
14. Knutti, R.; Masson, D.; Gettelman, A. Climate Model Genealogy: Generation CMIP5 and How We Got There. *Geophys. Res. Lett.* **2013**, *40* (6), 1194–1199. https://doi.org/10.1002/grl.50256.
15. McSweeney, C. F.; Jones, R. G.; Lee, R. W.; Rowell, D. P. Selecting CMIP5 GCMs for Downscaling over Multiple Regions. *Clim. Dyn.* **2015**, *44* (11–12), 3237–3260. https://doi.org/10.1007/s00382-014-2418-8.
16. Abramowitz, G.; Herger, N.; Gutmann, E.; Hammerling, D.; Knutti, R.; Leduc, M.; Lorenz, R.; Pincus, R.; Schmidt, G. A. ESD Reviews: Model Dependence in Multi-Model Climate Ensembles: Weighting, Sub-Selection and out-of-Sample Testing. *Earth Syst. Dyn.* **2019**, *10* (1), 91–105. https://doi.org/10.5194/esd-10-91-2019.
17. Srinivasa Raju, K.; Nagesh Kumar, D. Ranking General Circulation Models for India Using TOPSIS. *J. Water Clim. Chang.* **2015**, *6* (2), 288–299. https://doi.org/10.2166/wcc.2014.074.
18. Warszawski, L.; Frieler, K.; Huber, V.; Piontek, F.; Serdeczny, O.; Schewe, J. The Inter-Sectoral Impact Model Intercomparison Project (ISI–MIP): Project Framework. *Proc. Natl. Acad. Sci.* **2014**, *111* (9), 3228–3232. https://doi.org/10.1073/pnas.1312330110.
19. Khan, N.; Shahid, S.; Ahmed, K.; Ismail, T.; Nawaz, N.; Son, M. Performance Assessment of General Circulation Model in Simulating Daily Precipitation and Temperature Using Multiple Gridded Datasets. *Water (Switzerland)* **2018**, *10* (12). https://doi.org/10.3390/w10121793.
20. Shiru, M. S.; Shahid, S.; Chung, E.-S.; Alias, N.; Scherer, L. A MCDM-Based Framework for Selection of General Circulation Models and Projection of Spatio-Temporal Rainfall Changes: A Case Study of Nigeria. *Atmos. Res.* **2019**, *225* (March), 1–16. https://doi.org/10.1016/j.atmosres.2019.03.033.
21. Chandrashekar, G.; Sahin, F. A Survey on Feature Selection Methods. *Comput. Electr. Eng.* **2014**, *40* (1), 16–28. https://doi.org/10.1016/j.compeleceng.2013.11.024.
22. Talavera, L. An Evaluation of FIlter and Wrapper Methods for Categorical Clustering. **2005**.
23. Barfus, K.; Bernhofer, C. Assessment of GCM Capabilities to Simulate Tropospheric Stability

on the Arabian Peninsula. *Int. J. Climatol.* **2015**, *35* (7), 1682–1696. https://doi.org/10.1002/joc.4092.

24. Pierce, D. W.; Barnett, T. P.; Santer, B. D.; Gleckler, P. J. Selecting Global Climate Models for Regional Climate Change Studies. *Proc. Natl. Acad. Sci.* **2009**, *106* (21), 8441–8446. https://doi.org/10.1073/pnas.0900094106.
25. Ruan, Y.; Liu, Z.; Wang, R.; Yao, Z. Assessing the Performance of CMIP5 GCMs for Projection of Future Temperature Change over the Lower Mekong Basin. *Atmosphere (Basel).* **2019**, *10* (2), 93. https://doi.org/10.3390/atmos10020093.
26. Dudek, G. Tournament Searching Method to Feature Selection Problem. *Lect. Notes Comput. Sci. (including Subser. Lect. Notes Artif. Intell. Lect. Notes Bioinformatics)* **2010**, *6114 LNAI* (PART 2), 437–444. https://doi.org/10.1007/978-3-642-13232-2_53.
27. Hammami, D.; Lee, T. S.; Ouarda, T. B. M. J.; Le, J. Predictor Selection for Downscaling GCM Data with LASSO. *J. Geophys. Res. Atmos.* **2012**, *117* (17), 1–11. https://doi.org/10.1029/2012JD017864.
28. Sutha, K., Tamilselvi, J. . A Review of Feature Selection Algorithms for Data Mining Techniques. *Int. J. Comput. Sci. Eng.* **2015**, *7* (6), 63–67. http://www.enggjournals.com/ijcse/doc/IJCSE15-07-06-010.pdf
29. Perkins, S. E.; Pitman, A. J.; Holbrook, N. J.; McAneney, J. Evaluation of the AR4 Climate Models' Simulated Daily Maximum Temperature, Minimum Temperature, and Precipitation over Australia Using Probability Density Functions. *J. Clim.* **2007**, *20* (17), 4356–4376. https://doi.org/10.1175/JCLI4253.1.
30. Jiang, X.; Waliser, D. E.; Xavier, P. K.; Petch, J.; Klingaman, N. P.; Woolnough, S. J.; Guan, B.; Bellon, G.; Crueger, T.; DeMott, C.; et al. Vertical Structure and Physical Processes of the Madden-Julian Oscillation: Exploring Key Model Physics in Climate Simulations. *J. Geophys. Res. Atmos.* **2015**, *120* (10), 4718–4748. https://doi.org/10.1002/2014JD022375.
31. Min, S.-K.; Hense, A. A Bayesian Assessment of Climate Change Using Multimodel Ensembles. Part II: Regional and Seasonal Mean Surface Temperatures. *J. Clim.* **2007**, *20* (12), 2769–2790. https://doi.org/10.1175/jcli4178.1.
32. Shukla, J.; DelSole, T.; Fennessy, M.; Kinter, J.; Paolino, D. Climate Model Fidelity and Projections of Climate Change. *Geophys. Res. Lett.* **2006**, *33* (7), 3–6. https://doi.org/10.1029/2005GL025579.
33. Reichler, T.; Kim, J. How Well Do Coupled Models Simulate Today's Climate? *Bull. Am. Meteorol. Soc.* **2008**, *89* (3), 303–311. https://doi.org/10.1175/BAMS-89-3-303.
34. Shannon, C. E. A Mathematical Theory of Communication. **2001**, *5* (I), 365–395. https://doi.org/10.1007/3-540-45488-8_15.
35. Ma, C.-W.; Ma, Y.-G. Shannon Information Entropy in Heavy-Ion Collisions. **2018**. https://doi.org/10.1016/j.ppnp.2018.01.002.
36. Singh, B.; Kushwaha, N.; Vyas, O. P. A Feature Subset Selection Technique for High Dimensional Data Using Symmetric Uncertainty. *J. Data Anal. Inf. Process.* **2014**, No. November, 95–105. http://dx.doi.org/10.4236/jdaip.2014.24012.
37. Matemilola, S.; Adedeji, O. H.; Elegbede, I.; Kies, F. Mainstreaming Climate Change into the EIA Process in Nigeria: Perspectives from Projects in the Niger Delta Region. *Climate* **2019**, *7* (2). https://doi.org/10.3390/cli7020029.

Formatted: Font: Palatino Linotype, 10 pt, Font color: Auto

38. Amadi, A. N. Impact of Gas-Flaring on the Quality of Rain Water, Groundwater and Surface Water in Parts of Eastern Niger Delta, Nigeria. *J. Geosci. Geomatics* **2014**, *2* (3), 114–119. https://doi.org/10.12691/JGG-2-3-6.
39. Adejuwon, J. O. Rainfall Seasonality in the Niger Delta Belt , Nigeria. *J. Geogr. Reg. Plan.* **2012**, *5* (2), 51–60. https://doi.org/10.5897/JGRP11.096.
40. Amadi, A. N.; Olasehinde, P. I.; Nwankwoala, H. O. Hydrogeochemistry and Statistical Analysis of Benin Formation in Eastern Niger Delta , Nigeria. **2014**, *4* (3), 327–338. http://www.journalirjpac.com/index.php/IRJPAC/article/download/9121/16224/.
41. Etim U. U Ituen; A Folarin Alonge. Niger Delta Region of Nigeria, Climate Change and the Way Forward. *Bioenergy Eng. 11-14 Oct. 2009, Bellevue, Washingt.* **2009**, No. January 2009. https://doi.org/10.13031/2013.29162.
42. Prince C. Mmom, P. C. M. Vulnerability and Resilience of Niger Delta Coastal Communities to Flooding. *IOSR J. Humanit. Soc. Sci.* **2013**, *10* (6), 27–33. https://doi.org/10.9790/0837-1062733.
43. Amangabara, G.; Obenade, M. Flood Vulnerability Assessment of Niger Delta States Relative to 2012 Flood Disaster in Nigeria. *Am. J. Environ. Prot.* **2015**, *3* (3), 76–83. https://doi.org/10.12691/env-3-3-3.
44. Ologunorisa, T. E.; Tersoo, T. The Changing Rainfall Pattern and Its Implication for Flood Frequency in Makurdi, Northern Nigeria. *J. Appl. Sci. Environ. Manag.* **2006**, *10* (3), 97–102. http://www.bioline.org.br/pdf?ja06059.
45. Ologunorisa, T. E.; Adeyemo, A. Public Perception of Flood Hazard in the Niger Delta, Nigeria. *Environmentalist* **2005**, *25* (1), 39–45. https://doi.org/10.1007/s10669-005-3095-2.
46. Tawari-fufeyin, P., Paul, M., Godleads, A. O. Some Aspects of a Historic Flooding in Nigeria and Its Effects on Some Niger-Delta Communities. *Am. J. Water Resour.* **2015**, *3* (1), 7–16. https://doi.org/10.12691/ajwr-3-1-2.
47. Harris, I.; Jones, P. D.; Osborn, T. J.; Lister, D. H. Updated High-Resolution Grids of Monthly Climatic Observations - the CRU TS3.10 Dataset. *Int. J. Climatol.* **2014**, *34* (3), 623–642. https://doi.org/10.1002/joc.3711.
48. Jones, P.D.; Harris, I. C. *Climatic Research Unit (CRU) Time-Series Datasets of Variations in Climate with Variations in Other Phenomena. NCAS British Atmospheric Data Centre*; 2008. http://catalogue.ceda.ac.uk/uuid/3f8944800cc48e1cbc29a5ee12d8542d.
49. Ashraf Vaghefi, S.; Abbaspour, N.; Kamali, B.; Abbaspour, K. C. A Toolkit for Climate Change Analysis and Pattern Recognition for Extreme Weather Conditions – Case Study: California-Baja California Peninsula. *Environ. Model. Softw.* **2017**, *96* (October), 181–198. https://doi.org/10.1016/j.envsoft.2017.06.033.
50. Hassan, I.; Kalin, R. M.; White, C. J.; Aladejana, J. A. Evaluation of Daily Gridded Meteorological Datasets over the Niger Delta Region of Nigeria and Implication to Water Resources Management. *Atmos. Clim. Sci. , SCRIP* **2020**. https://www.scirp.org/journal/paperinformation.aspx?paperid=97271.
51. Hempel, S.; Frieler, K.; Warszawski, L.; Schewe, J.; Piontek, F. A Trend-Preserving Bias Correction – The ISI-MIP Approach. *Earth Syst. Dyn.* **2013**, *4* (2), 219–236. https://doi.org/10.5194/esd-4-219-2013.
52. Wang, L.; Ranasinghe, R.; Maskey, S.; van Gelder, P. H. A. J. M.; Vrijling, J. K. Comparison of Empirical Statistical Methods for Downscaling Daily Climate Projections from CMIP5 GCMs:

Formatted: Font: Palatino Linotype, 10 pt, Font color: Auto

A Case Study of the Huai River Basin, China. *Int. J. Climatol.* **2016**, *36* (1), 145–164. https://doi.org/10.1002/joc.4334.

53. Piao, M.; Piao, Y.; Lee, J. Y. Symmetrical Uncertainty-Based Feature Subset Generation and Ensemble Learning for Electricity Customer Classification. *Symmetry (Basel).* **2019**, *11* (4), 4–13. https://doi.org/10.3390/sym11040498.
54. Adami, C. Information Theory in Molecular Biology. *Phys. Life Rev.* **2004**, *1* (1), 3–22. https://doi.org/10.1016/j.plrev.2004.01.002.
55. Shreem, S. S.; Abdullah, S.; Nazri, M. Z. A. Hybrid Feature Selection Algorithm Using Symmetrical Uncertainty and a Harmony Search Algorithm. *Int. J. Syst. Sci.* **2016**, *47* (6), 1312–1329. https://doi.org/10.1080/00207721.2014.924600.
56. Roszkowska, E. Rank Ordering Criteria Weighting Methods-a Comparative Overview 2 5. *OPTIMUM. Stud. Ekon.* **2013**, *5* (5), 65. https://pdfs.semanticscholar.org/f983/e8c4eb7d7c30694dd72c5849dd6fee8a5c79.pdf
57. Balinski, M.; Laraki, R. *Majority Judgment vs. Majority Rule*; Springer Berlin Heidelberg, 2019. https://doi.org/10.1007/s00355-019-01200-x.
58. Mehrotra, R.; Sharma, A. Correcting for Systematic Biases in Multiple Raw GCM Variables across a Range of Timescales. *J. Hydrol.* **2015**, *520* (January), 214–223. https://doi.org/10.1016/j.jhydrol.2014.11.037.
59. Beyer, R.; Krapp, M.; Manica, A. A Systematic Comparison of Bias Correction Methods for Paleoclimate Simulations. *Clim. Past Discuss.* **2019**, No. February, 1–23. https://doi.org/10.5194/cp-2019-11.
60. Xu, Y. Hydrology and Climate Forecasting R Package for Data Analysis and Visualization. 2018. https://cran.r-project.org/web/packages/hyfo/vignettes/hyfo.pdf.
61. Moriasi, D. N.; Arnold, J. G.; Liew, M. W. Van; Bingner, R. L.; Harmel, R. D.; Veith, T. L. Model Evaluation Guidelines for Systematic Quantification of Accuracy in Watershed Simulations. *Am. Soc. Agric. Biol. Eng.* **2007**, *50* (3), 885–900. http://citeseerx.ist.psu.edu/viewdoc/download?doi=10.1.1.532.2506&rep=rep1&type=pdf
62. Motovilov, Y. G.; Gottschalk, L.; Engeland, K.; Rodhe, A. Validation of a Distributed Hydrological Model against Spatial Observations. **1999**, *99*. http://dx.doi.org/10.1016/S0168-1923(99)00102-1.
63. Srinivasa Raju, K.; Sonali, P.; Nagesh Kumar, D. Ranking of CMIP5-Based Global Climate Models for India Using Compromise Programming. *Theor. Appl. Climatol.* **2017**, *128* (3–4), 563–574. https://doi.org/10.1007/s00704-015-1721-6.
64. Krinner, G.; Germany, F.; Shongwe, M.; Africa, S.; France, S. B.; Uk, B. B. B. B.; Germany, V. B.; Uk, O. B.; France, C. B.; Uk, R. C.; et al. Long-Term Climate Change: Projections, Commitments and Irreversibility. *Clim. Chang. 2013 Phys. Sci. Basis Work. Gr. I Contrib. to Fifth Assess. Rep. Intergov. Panel Clim. Chang.* **2013**, *9781107057*, 1029–1136. https://doi.org/10.1017/CBO9781107415324.024.
65. Expósito, F. J.; González, A.; Pérez, J. C.; Díaz, J. P.; Taima, D. High-Resolution Future Projections of Temperature and Precipitation in the Canary Islands. *J. Clim.* **2015**, *28* (19), 7846–7856. https://doi.org/10.1175/JCLI-D-15-0030.1.
66. Rangwala, I.; Miller, J. R. Climate Change in Mountains: A Review of Elevation-Dependent Warming and Its Possible Causes. *Clim. Change* **2012**, *114* (3–4), 527–547.

Formatted: Font: Palatino Linotype, 10 pt, Font color: Auto

https://doi.org/10.1007/s10584-012-0419-3.

67. Martín, J. L.; Bethencourt, J.; Cuevas-Agulló, E. Assessment of Global Warming on the Island of Tenerife, Canary Islands (Spain). Trends in Minimum, Maximum and Mean Temperatures since 1944. *Clim. Change* **2012**, *114* (2), 343–355. https://doi.org/10.1007/s10584-012-0407-7.
68. Agumagu, O.; Todd, M. Modelling the Climatic Variability in the Niger Delta Region : Influence of Climate Change on Hydrology. *Earth Sci. Clim. Chang.* **2015**, *6* (6). https://doi.org/10.4172/2157-7617.1000284.
69. Obroma Agumagu, O. A. Projected Changes in the Physical Climate of the Niger Delta Region of Nigeria. *SciFed J. Glob. Warm.* **2018**. https://pdfs.semanticscholar.org/c5e7/17ebcd21acd09109553f3c11804f94ece611.pdf?_ga=2.9422967.312418545.1579023164-1793679239.1552909823.
70. Ike, P. C.; Emaziye, P. O. An Assessment of the Trend and Projected Future Values of Climatic Variables in Niger Delta Region , Nigeria. **2012**, *4* (2), 165–170. https://www.researchgate.net/profile/Pius_Ike/publication/268202347_An_Assessment_of_the_Trend_and_Projected_Future_Values_of_Climatic_Variables_in_Niger_Delta_Region_Nigeria/links/5b008a9ba6fdccf9e4f56f9a/An-Assessment-of-the-Trend-and-Projected-Future-Values-of-Climatic-Variables-in-Niger-Delta-Region-Nigeria.pdf

Formatted: Font: Palatino Linotype, 10 pt, Font color: Auto